Department of Precision and Microsystems Engineering

Damping Analysis of Reset Control Systems: an Analytical Approach

Mees Vanderbroeck

Report no : 2022.087
Coach : Nima Karbasizadeh
Professor : Dr. S Hassan HosseinNia
Specialisation : Mechatronic System Design
Type of report : Master thesis
Date : 8 December 2022

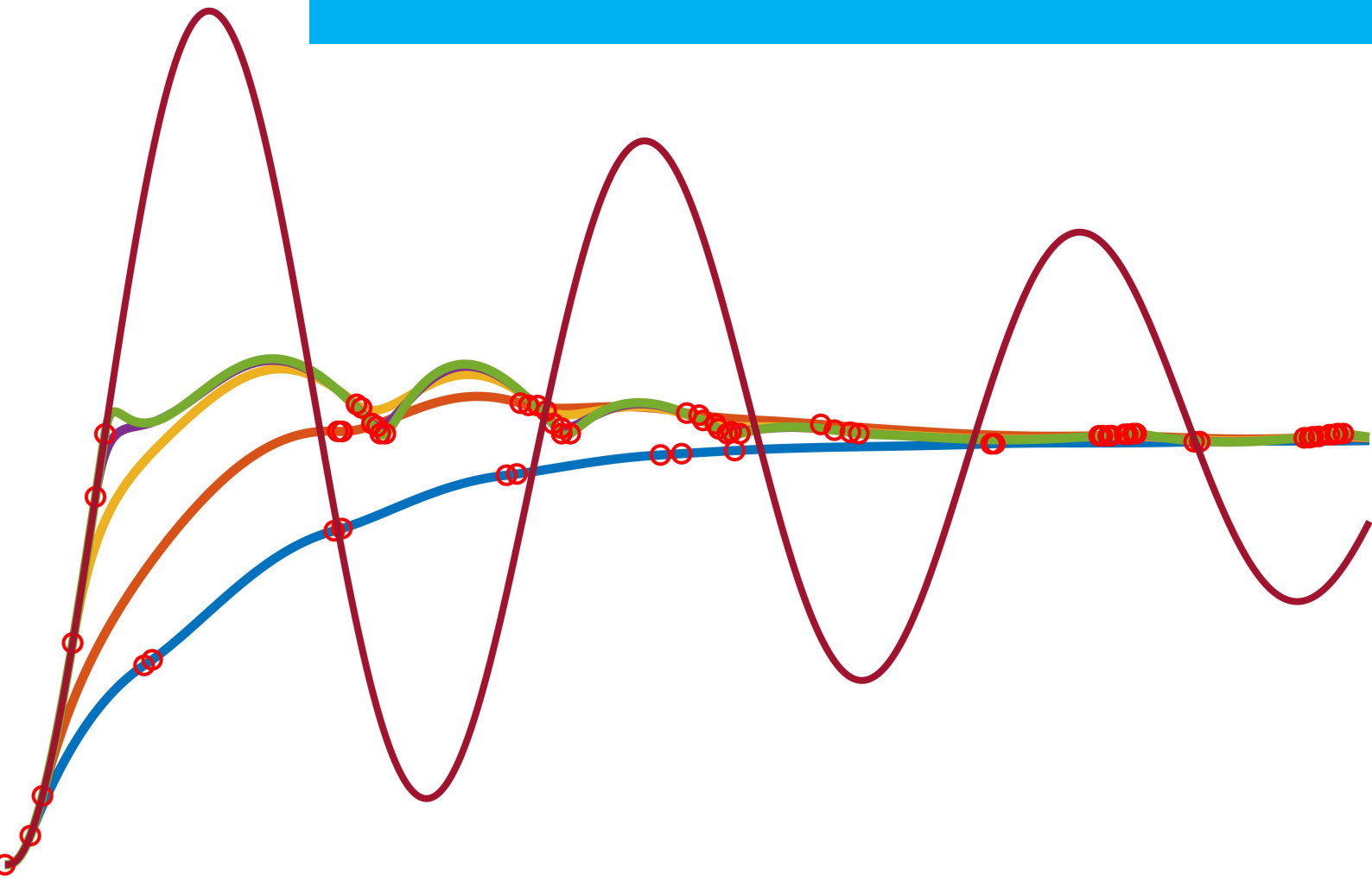

TU Delft Delft University of Technology

Challenge the future

Damping Analysis of Transient Response in Reset Control Systems: an Analytical Approach

by

M. Vanderbroeck

to obtain the degree of Master of Science
at the Delft University of Technology
to be defended publicly on Thursday 22 december, 2022 at 9:00.

Student number: 4556763
Project duration: September 1, 2021 – December 22, 2022
Thesis committee:

Dr. ir. S. Hassan HosseinNia,	TU Delft, supervisor
Ir. Nima Karbasizadeh,	TU Delft, daily supervisor
Dr. ir. Dimitris Boskos,	TU Delft

TU Delft

Abstract

The high-tech industry continuously pushes the boundaries of controller performance to achieve faster and more precise machines. Currently, linear control is the standard in the industry. These controllers suffer from the waterbed effect and Bode's phase/gain relation, which impose inherent limitations on the precision and robustness of the system. Reset control is a popular strategy to get around these limitations and improve performance. The damping in reset control systems is not only determined by the phase margin of the system but is also dependent on the exact controller element sequence. Currently, finding the optimal controller sequence is done through simulation of the step response. However, this fails to provide insight into the underlying cause of the additional damping achieved by specific controller configurations. This thesis proposes an analytical approach to analyze the damping of the transient response reset control systems. The analytical analysis provides a better understanding of sequence-dependent damping and assists in controller design. First, the analytical expressions of the step response and states of the system are derived, which are used to define the system's energy. The step response and energy equations are used to characterize the damping in a reset control system. To show the value of the proposed method, the damping in a reset control system is assessed as an illustrative example. It is found that when a lead is in front of a reset element, the reset controller can provide more damping because it reduces the oscillatory content in the step response.

M. Vanderbroeck
Delft, December 8, 2022

Preface

This thesis is the final part of the High-Tech Engineering track of the Mechanical Engineering master at the TU Delft. The project was done as part of the Mechatronic System Design group at the Precision and Microsystem Engineering Department. After enjoying the Mechatronic System Design course, Hassan HosseinNia and Nima Karbasizadeh suggested considering reset control as the topic of my thesis project.

I want to thank both of my supervisors for the guidance they provided. Nima has helped me tremendously with our numerous (zoom) meetings. During the discussions, he always had a critical eye, which helped me improve this thesis's quality. Hassan provided a lot of experience and enthusiasm during this project. Thank you for helping me better define this project's scope and what to do next. Moreover, I want to thank both of them for their patience. Last year was quite a challenge with multiple periods of medical issues. Despite the struggle, they were always supportive and helped me progress.

Finally, I want to thank my friends and family for the support they gave me last year. They motivated me to continue and finish this project successfully.

M. Vanderbroeck
Delft, December 8, 2022

Contents

1 Introduction

1.1. Introduction

Motion control systems are essential in the current technology-driven society. Machines that can create the desired motion are found in many industries. These devices range from simple assembly-line systems to the most advanced high-tech machines. The latter regards motion control systems, which are required to operate at micro- and nanometer precision to obtain the small features in high-tech products. PID control is the most common control method to meet the set precision requirements. Through the implementation of loop-shaping and feed-forward techniques, high bandwidth, high precision, and robust motion control can be achieved. However, this linear control method has its limitations. Bode's Phase/Gain relationship and the waterbed effect impose limitations on every LTI controller [1, 2]. The Phase/Gain relationship limits the level of robustness and precision that can be reached simultaneously. Moreover, the waterbed effect will impose a trade-off between the amount of noise attenuation and disturbance rejection provided by linear control. The demands on controller performance in the high-tech industry are approaching the limit of achievable linear controller performance. Therefore, there is a need for other strategies to meet the demands of the industry.

Reset control is a popular strategy to get around the limitations of linear control. The technique involves resetting one or multiple controller states when a specific condition is met. Reset control is mainly popular due to its compatibility with the PID architecture and loop-shaping techniques. Often reset elements replaces a linear lag element in a conventional LTI controller. The first application of reset control was the introduction of a nonlinear integrator discovered by Clegg in [3]. This novel element reduced the phase lag of its linear counterpart significantly. Since then, many reset elements and architectures have been introduced [4–9]. The main advantage of reset control is the ability to reduce phase lag. In literature, it is shown that reset control can provide a significant improvement in controller performance in the frequency domain and steady-state response [10–18].

Moreover, the transient performance can also be improved with the reduction and prevention of overshoot [4, 16, 17, 19]. The overshoot reduction can partially be attributed to an increase in phase margin. In [20], it is shown that also the controller configuration affects the transient response and can be used to improve transient performance. Therefore, the transient performance is determined by more than the first-order frequency response. In [7, 20], it is shown that placing a lead before a reset element can provide additional damping to the system compared to other controller sequences. The step response in these studies is found numerically to tune the control element sequence for transient performance. However, the simulation cannot provide insight into the underlying cause of the damping induced by the different controller configurations. When the damping in reset control systems could be analyzed analytically, the source of the additional damping could be better understood and used to aid in controller design for transient performance.

1.2. Thesis outline

This thesis aims to investigate how reset control dampens the transient response of a motion control system apart from providing additional phase margin. First, a literature review is done on how the transient performance can be improved with the implementation of reset control in Section 2. As a result, the research goal and approach are formulated in Section 3. This research's main contribution is provided in a paper format in Section 4. Here, an analytical approach to the damping analysis in reset control systems with mass plants is proposed. The value of the approach is shown by analyzing the damping in a reset control system as an illustrative example. Here the influence of lead placement on the damping of the step response is investigated. Conclusions of this work are stated in Section 5. Finally, the recommendations for future research are given in Section 6. More details on this work can be found in Appendix A-C.

2

Literature review: Improving the Transient Performance of Reset Control Systems

This section is dedicated to a literature review on improving the transient performance of reset control systems. This review in paper format shows the different ways that reset control can influence the transient response of a motion control system. The main goal of this review is to identify the problem statement and research goals for this study. The problem statement and research goals resulting from this review are stated in Section 3.

The review paper introduces reset control's relevancy in general and transient performance in particular. Next, the review provides some preliminary knowledge. After that, the influence of reset control on transient behavior is stated. The connection between transient and frequency response in reset control is discussed. After, the direct impact of the control parameters of reset controllers on the transient performance is shown. Finally, the review is concluded, and the research gap is formulated.

Literature Review: Improving the Transient Performance of Reset Control Systems

Mees Vanderbroeck* Nima Karbasizadeh* S. Hassan HosseinNia*

***Abstract*— The high-tech industry is always looking into ways to improve the precision and speed of its products. Linear controllers suffer from the fact that they are inherently bounded by Bodes phase/gain relationship and the waterbed effect. As a result, there is a limit on the amount of precision and robustness that can be achieved. Nonlinear reset controllers provide a method to omit this limitation and can further improve controller performance compared to the industry standard PID control systems. The relation between the frequency and transient response is not as straightforward in nonlinear control as in linear control. The damping in a reset control system cannot be derived solely from the first-order frequency response. Therefore, the transient response is hard to predict and is often just simulated numerically. Which makes tuning to improve transient response performance hard. In this study, an overview is given of how reset control can improve transient performance. Furthermore, this work proposes to develop an analytical approach to analyze the damping of the transient response in reset control systems. An exact relation between the control parameters and the transient response would allow for more systematic tuning methods of reset systems to be developed.**

Keywords: Non-linear control, Reset control (RC), Transient response

I. Introduction

The high-tech industry continuously strives to enhance controller performance in precision motion systems. By increasing the precision and speed of these systems, product quality and capacity can be increased. Moreover, product dimensions can be decreased, which is especially relevant for the semiconductor industry. Current computer chips already contain features on the nanometer scale, so control precision needs to be sufficient for the production of these features. To increase speed and precision in the transient part of the response, the aim is to decrease rise time, overshoot and settling time.

Currently, linear PID control is the industry standard for controlling precision motion systems. Due to the growing demands on precision and speed, the industry is approaching the performance limit of linear control. In linear control, the phase and gain of the system are related to each other by (1), called Bode's Phase-Gain relation.

$$\angle G(j\omega) \simeq n \times 90^\circ \tag{1}$$

n represents the slope of the magnitude of $G(j\omega)$. This relation imposes a limitation on the achievable bandwidth of the system when certain stability margins are required. In other words, robustness, precision and speed can only be improved simultaneously to a certain degree in linear systems [1]. Moreover, linear controllers suffer from the waterbed effect [2], which is imposed by Bode's sensitivity integral (2). This equation shows that the reduction in sensitivity at a certain frequency necessarily causes an increase in sensitivity at another frequency. This means that high-frequency noise attenuation and low-frequency disturbance rejection cannot be improved simultaneously.

$$\int_0^\infty \ln |S(j\omega)| d\omega = 0 \tag{2}$$

Both restrictions can be bypassed by implementing nonlinear control. Reset control is one of the existing nonlinear controller types that has been gaining popularity in recent years. Compared to other nonlinear control methods, the advantage of reset control is its compatibility with PID control and loop shaping techniques. Reset controllers contain elements that will (partially) reset their states when a certain reset condition is met. Clegg introduced the first reset element in [3]. He showed that a resetting integrator could decrease phase lag compared to a linear integrator of 52°. Many new reset elements have since been introduced and implemented [4]–[9]. In literature, it is shown that reset control can provide a significant increase in control performance in the frequency domain and steady-state performance [10]–[18]. The main advantage of reset control is the reduction of phase lag or even providing phase lead to a system.

The reduction of phase lag can be used to increase the phase margin of reset control systems. The increase in phase margin would largely determine the overshoot in a linear system [2]. However, the connection between the transient and frequency response is not as straightforward for nonlinear control since higher-order harmonics are present. Moreover, different controller sequences cause different transient responses in reset control even when the phase margin is kept constant [19]. For example, when a lead element is used before the reset element, beneficial transient behavior can be created compared to the lead element after the reset. Clear guidelines on systematically tuning reset controllers for improvements in transient performance directly are scarce.

In this paper, an overview is given of the work that is done on the influence of reset control on the transient response

* Department of Precision and Microsystem Engineering, Delft University of Technology, Delft, The Netherlands

of the system. Moreover, a research topic is proposed on how to gain insight into the effect of control parameters and sequences on the step response. By formulating an analytical approach to analyze the damping in reset control systems, more systematic tuning methods for transient performance could be developed. The remainder of the paper is structured as follows. In section II, the prior knowledge on reset control and transient response are discussed. The (dis)advantages of reset control on transient performance found in the literature are stated in section III. In section IV, the relation between reset systems' frequency and transient response is explored. The influence of reset control parameters on transient performance is shown in section V. The review's conclusion and the research goal for the rest of the thesis are provided in section VI.

II. Preliminaries

A. Definition general reset controller

Reset systems can generally be written as (3).

$$\Sigma_R := \begin{cases} \dot{x}_r = A_r x_r(t) + B_r e(t), & \text{if} \quad e(t) \neq 0 \\ x_r(t^+) = A_\rho x_r(t), & \text{if} \quad e(t) = 0 \\ u(t) = C_r x_r(t) + D_r e(t) \end{cases} \tag{3}$$

Matrices A_r, B_r, C_r, D_r describe the state-space representation of the Base Linear System (BLS) of the reset system. The BLS is equivalent to the reset system without resetting action. Matrix A_ρ determines the amount of reset when the reset condition is met. For now, the most common reset condition $e(t) = 0$ is considered. $x_r(t)$, $e(t)$, and $u(t)$ describe the reset controller states, controller input, and controller output, respectively.

B. Describing functions

Loop shaping techniques are the industry standard for tuning controllers. This technique is based on the frequency response of the system. Unfortunately, the frequency domain behaviour of nonlinear control systems cannot be analysed by conventional linear frequency response function (FRF) analysis since the response to a sinusoidal input is not sinusoidal for a reset element. Therefore, the frequency response of reset systems needs to be analysed differently. In literature, this is mostly done using Higher Order Sinusoidal Input Describing Function (HOSIDF) analysis introduced by [20]. In most cases, loop shaping method based on the first harmonic is used to tune the controller in the frequency domain. This could be problematic when the magnitude of the higher-order harmonics is close to the magnitude of the first harmonic since the first harmonic will not capture the overall frequency domain behaviour well.

In [21], the HOSIDFs for a general reset controller are obtained:

$$G_n(j\omega) = \begin{cases} C_r(j\omega I - A_r)^{-1}(I + j\Theta_\rho(\omega))B_r + D_r & n = 1 \\ C_r(nj\omega I - A_r)^{-1}(I + j\Theta_\rho(\omega))B_r & \text{odd } n \geq 2 \\ 0 & \text{even } n \geq 2 \end{cases} \tag{4}$$

Where,

$$\begin{aligned} \Theta_\rho(\omega) &= \frac{2\omega^2}{\pi}\Delta(\omega)(\Gamma(\omega) - \Lambda^{-1}) \\ \Gamma(\omega) &= \Delta_\rho(\omega)^{-1} A_\rho \Delta(\omega)\Lambda(\omega)^{-1} \\ \Delta_\rho(\omega) &= I + A_\rho e^{\frac{A_r \pi}{\omega}} \\ \Delta(\omega) &= I + e^{\frac{A_r \pi}{\omega}} \\ \Lambda(\omega) &= \omega^2 I + A_r \end{aligned} \tag{5}$$

C. Reset elements

1) Clegg integrator: The Clegg Integrator (CI) was the first reset element introduced by [3]. A reduction of $52°$ phase lag can be achieved by applying reset to a linear integrator. The state-space representation of a CI can be written to the form in (3), where:

$$A_r = 0, B_r = 1, C_r = 1, D_r = 0, A_\rho = 0 \tag{6}$$

2) (Generalized) First/Second Order Reset Element: As an extension of the CI, the First Order Reset Element (FORE) was introduced by [4]. FORE essentially is a first-order low-pass filter with resetting action. It provides more design freedom by changing the filter's corner frequency ω_r. The conventional FORE in [4] fully resets when the reset condition is met. The generalized FORE (GFORE), introduced in [20], also allows for a partial reset of the FORE. The amount of reset is determined by the value of γ. In a conventional FORE, γ is fixed to zero. Note that the real corner frequency of the reset filter is not exactly equal to ω_r. For different values of γ, the real corner frequency shifts. This could be accounted for, as done in [6]. The state-space representation of GFORE can be written to the form in (3), where:

$$A_r = -\omega_r, B_r = \omega_r, C_r = 1, D_r = 0, A_\rho = \gamma \tag{7}$$

The reset equivalent of a second-order low-pass filter is called a Second Order Reset Element (SORE) and was introduced by [5]. The additional control parameter β_r can be used to change the damping of the element. As with the FORE, the conventional SORE only regards full reset. The generalized SORE (GSORE) also allows partial reset determined by γ_1 and γ_2. Both parameters individually determine the amount of reset of each separate controller state. A state-space representation of GSORE can be written to the form in (3), where:

$$\begin{aligned} A_r = \begin{bmatrix} 0 & 1 \\ -\omega_r^2 & -2\beta_r\omega_r \end{bmatrix}, B_r = \begin{bmatrix} 0 \\ \omega_r^2 \end{bmatrix}, \\ C_r = \begin{bmatrix} 1 & 0 \end{bmatrix}, D_r = [0], A_\rho = \begin{bmatrix} \gamma_1 & 0 \\ 0 & \gamma_2 \end{bmatrix} \end{aligned} \tag{8}$$

In contrast to linear control, the exact state-space representation of a reset system does influence the output of the system in nonlinear control [22]. In other words, the output depends on the exact configuration of the control elements. Therefore, the superposition principle does not apply [23].

Use the correct representation to describe the actual reset control system.

Both GFORE and GSORE can also be described in transfer function form:

$$GFORE(s) = \frac{1}{s/\omega_r + 1}^{\gamma} \tag{9}$$

$$GSORE(s) = \frac{1}{(s/\omega_r)^2 + (2s\beta_r/\omega_r) + 1}^{\gamma_1,\gamma_2} \tag{10}$$

The arrow crossing the equation shows that the element is a reset element.

3) Constant in Gain Lead in Phase: The Constant in gain Lead in phase (CgLp) element was introduced by [6]. Most reset elements can provide a reduction of phase lag when it replaces their linear counterpart. A CgLp element can also provide phase lead to a system at an extensive range of frequencies.

A CgLp element combines a reset lag filter R with a linear lead filter L of equal order. The reset lag filter can be a GFORE or GSORE. These filters can be described as follows:

$$R(s) = \frac{1}{(s/\omega_{r\alpha})^2 + (2s\beta_r/\omega_{r\alpha}) + 1}^{\gamma} \text{ or } \frac{1}{s/\omega_{r\alpha} + 1}^{\gamma} \tag{11}$$

and

$$L(s) = \frac{(s/\omega_r)^2 + (2s\beta_r/\omega_r) + 1}{(s/\omega_f)^2 + (2s/\omega_f) + 1} \quad \text{or} \quad \frac{s/\omega_r + 1}{s/\omega_f + 1} \tag{12}$$

ω_r and ω_f are the lead filter's corner frequency and termination frequency, respectively. $\omega_{r\alpha} = \omega_r/\alpha$ is the corner frequency correction of the reset element to match the corner frequency ω_r of the lead filter. For frequencies between ω_r and ω_f, the CgLp provide phase lead with unity gain, as seen in Fig. 1. State-space matrices of a CgLp element consisting of a GFORE are as follows:

$$\begin{aligned} A_r &= \begin{bmatrix} -\omega_{r\alpha} & 0 \\ -\omega_f & \omega_f \end{bmatrix}, B_r = \begin{bmatrix} \omega_{r\alpha} \\ 0 \end{bmatrix}, \\ C_r &= \begin{bmatrix} \frac{\omega_f}{\omega_r} & (1 - \frac{\omega_f}{\omega_r}) \end{bmatrix}, D_r = [0], A_\rho = \begin{bmatrix} \gamma & 0 \\ 0 & 1 \end{bmatrix} \end{aligned} \tag{13}$$

Note that this state-space representation describes a CgLp where the lead element is after the reset element. The realization should be changed when the order is switched.

D. Transient response of a system

The transient response of a system is the first part of the time response to a change to the equilibrium position. The transient response is the temporary part of the time response and will vanish over time. This paper will only regard the system's step response to determine the transient response performance.

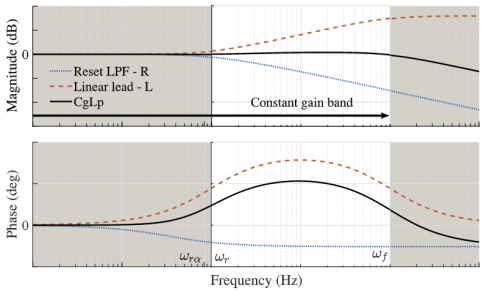

Fig. 1: Frequency response of a CgLp element [6].

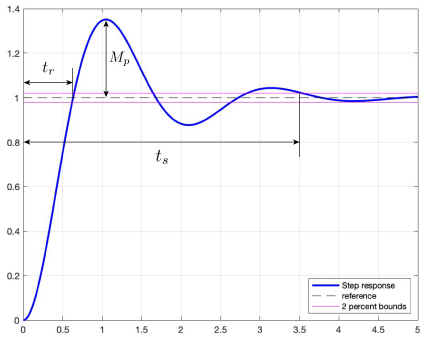

Fig. 2: Step response with rise time, overshoot and settling time definition.

To characterize the transient response performance, the following metrics are considered (see also Fig. 2):

- Rise time, t_r
  The time it takes the signal to reach the new reference value for the first time.
- Overshoot, M_p
  The maximum amount the signal exceeds the reference value
- Settling time, t_s
  The time it takes the signal to stay within a certain error band with respect to the reference (often 2% of reference value)

In control, the aim is to minimize rise time, overshoot and settling time to improve controller performance.

III. Transient Performance of Reset Control Systems

A. Transient response benefiting from reset

In literature, the advantage of reset control for transient performance is often shown through simulation or experiments. The first paper to show the benefit was [4], which used a FORE to decrease overshoot. In [17] it is shown that a FORE can satisfy a certain set of rise time and overshoot constraints for an integrator plant, whereas a linear controller cannot satisfy both constraints simultaneously. [16] shows a decrease in overshoot and settling time for a FORE that is compared to its BLS, see Fig. 3. In [10], the transient performance of a FORE

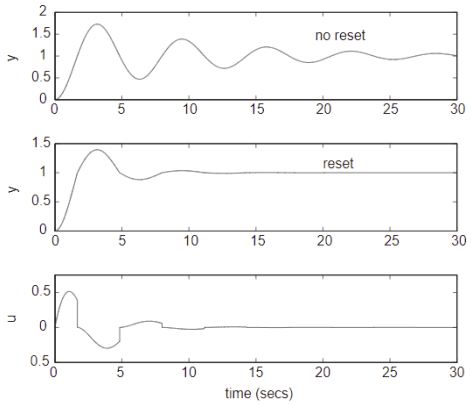

Fig. 3: Step response of linear and reset system [16].

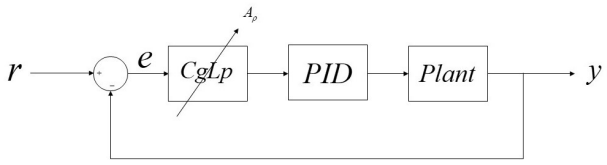

Fig. 4: Control scheme CgLp with PID.

controlling a second-order plant is defined analytically. From these equations [10] shows that the reset decreases overshoot and settling time for equal rise time compared to its BLS.

The improvement in transient performance can partially be contributed to the additional phase compensation that the nonlinear elements provide. However, this is not the only cause of the performance improvement. To show this consider a linear PID controller and a reset control system containing a GFORE CgLp element (see (13)) and a PID in series, controlling a mass-spring-damper system. The controller scheme of this reset system can be seen in Fig. 4. Both controllers are tuned to have a phase margin of approximately $40°$. Tuning is done according to the guidelines provided in [6]. The first-order frequency response of both systems can be seen in Fig. 5.

If both controllers were linear, one would expect both systems to result in a similar overshoot since the phase margin is equal for both. However, in Fig. 6 is shown that the reset system has considerably reduced overshoot. This implies that the reduction in overshoot of a reset system is not only caused by the reduction of phase lag since this was kept constant in this example.

In [24], the same behaviour is observed. Here, reset control is used to approximate complex-order control (CLOC) (introduced in [9]). The performance of the CLOC framework in [24] is experimentally verified by comparing a linear PID to a PI-CgLp, a PID-CgLp and 2 CLOC

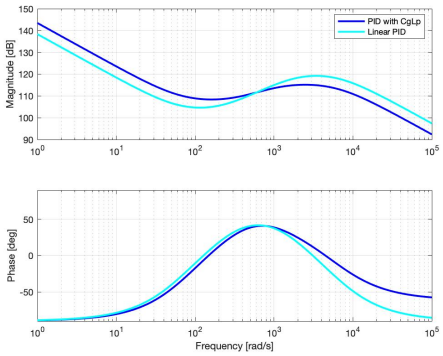

Fig. 5: First order open-loop frequency response of Linear and Reset controller.

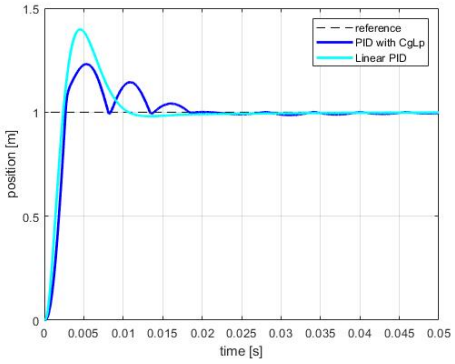

Fig. 6: Step response of CgLp+PID and PID control systems.

controllers, which are all designed to have the same phase margin, like in Fig. 7. In Fig. 8, it is shown that all four reset systems decrease the overshoot compared to the linear PID controller, even when the phase margin is equal for all. In short, different properties of reset controllers other than phase margin should be considered to capture the transient performance of the system fully.

B. Disadvantages of reset control for transient response

Higher-order harmonics in reset control systems can deteriorate the performance in the frequency domain [6], [25], [26]. Also, transient performance can suffer from the introduction of higher-order harmonics. Limit cycles are a common problem in reset systems. Limit cycles are persistent oscillations in the time response of the system. This undesired behaviour mostly occurs when model uncertainties are present, shown in [27]. However, reset systems without model uncertainties can also lead to limit cycles. In [19], the occurrence of limit cycles is shown for reset PI controlling a first-order plant. The step response can be seen in Fig. 9. [28] and [29] provide methods to analyse the presence, properties and stability of limit cycles.

Fortunately, there are multiple strategies to prevent the generation of limit cycles. The higher-order harmonics can

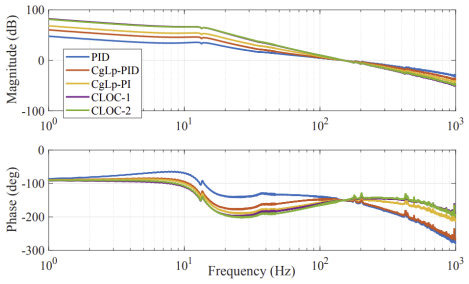

Fig. 7: Frequency response of linear PID, PID-CgLp, PI-CgLp and 2 CLOC, all tuned for the same phase margin [24].

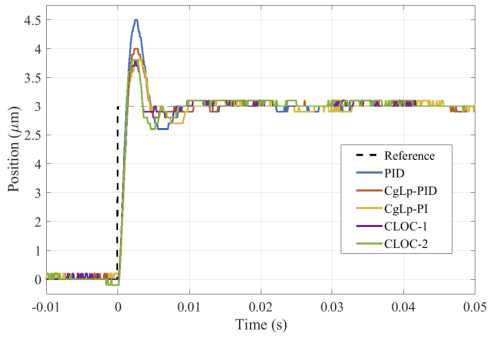

Fig. 8: Transient response of linear PID, PID-CgLp, PI-CgLp and 2 CLOC, all tuned for the same phase margin [24].

be reduced in magnitude by decreasing the amount of nonlinearity in the system. Therefore, suppressing the limit cycles. For example, [27] proposes using a PI+CI controller as a possible solution.

IV. Relation Transient and Frequency Response

Over time, different reset elements have been introduced, which aim to increase the phase the reset controller provides compared to its linear counterpart. Moreover, control strategies are introduced that are aiming to suppress higher-order harmonics at certain frequencies. These techniques regard shaping filters on the reset line, adding filters in front/after the reset element, changing the amount of reset and changing the reset condition [1], [5]–[8], [30], [31]. This body of research can be used to tune reset controllers for different applications in the frequency domain.

In linear control, one can estimate the transient performance by looking at the system's stability margins, bandwidth and sensitivity. Unfortunately, a method for predicting the transient performance of reset systems based on the frequency response does not yet exist. To show this, consider multiple PI-CgLp controllers retrieved from [19]. The controllers all consist of a GFORE reset element, a PI lag element and a linear lead element. The sequence of the elements is changed for each controller. One of the controller schemes is shown in Fig. 10. The first-order

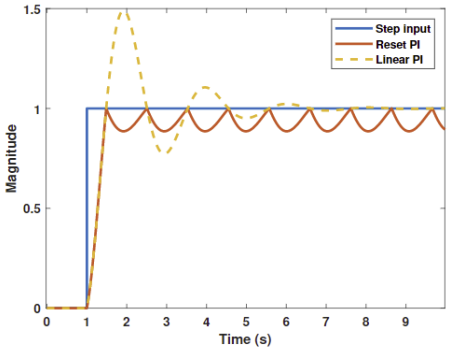

Fig. 9: Limit cycles in reset system without model uncertainties [19].

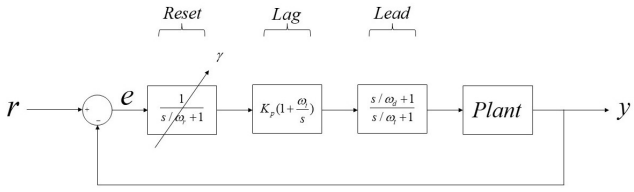

Fig. 10: PI-CgLp control scheme with the sequence: Reset-Lag-Lead.

frequency response of all controllers is equal, see Fig. 11. Therefore, similar rise time, overshoot and settling time are expected for all sequences in linear control.

However, the step responses in Fig. 12 show that all sequences lead to a different transient performance. Interestingly, the systems with the lead element in front of the reset element show a significantly different response than the other two configurations. In these configurations, the reset instances depend on a linear combination of the error and the derivative of the error. Therefore, resets can happen even when the system's output is not equal to the reference. This leads to a less intuitive response, but it could be beneficial when a no-overshoot response is

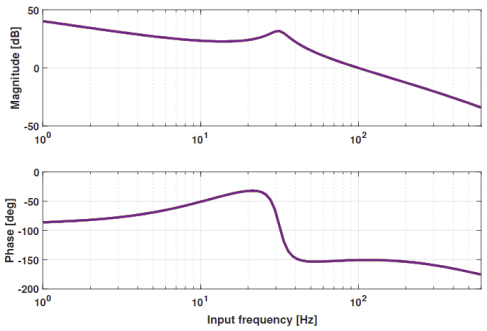

Fig. 11: First order frequency response of the system for different PI-CgLp configurations [19].

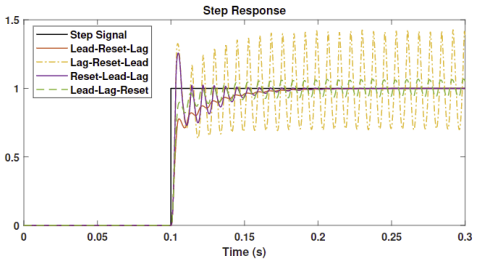

Fig. 12: Step Response of system for different PI-CgLp configurations [19].

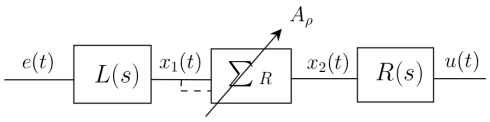

Fig. 13: Continuous Reset architecture with lead element $L(s) = \frac{s/\omega_l+1}{s/\omega_h+1}$, before the reset element and lag element $R(s) = \frac{1}{s/\omega_l+1}$ [7].

desired. However, more insight is needed into when the reset instances happen. In short, Fig. 12 shows that the transient response of a reset system cannot be predicted based only on the first-order frequency response.

Similarly, [7] can provide insight into the connection between the sensitivity and the transient performance of reset systems. In [7], an architecture called a Continuous Reset (CR) element is introduced, which provides reset elements with a continuous output signal. The control scheme is shown in Fig. 13. The architecture's performance is illustrated by comparing a CgLp to a CR CgLp. It is shown that when both controllers have the same phase margin and peak of sensitivity, the CR CgLp leads to a significantly lower overshoot, see Fig. 14. Therefore, the transient performance is (also) not solely determined by the peak of sensitivity.

Overall, the transient performance of reset systems is hard to predict since it depends on many factors like phase margin, controller sequence, bandwidth, sensitivity and higher-order harmonics. To tune for frequency and transient performance

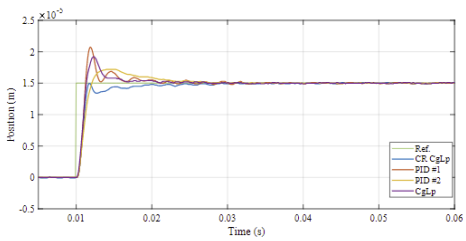

Fig. 14: Step response of similarly tuned CR CgLp and CgLp controllers [7].

simultaneously, more insight is needed into the connection between the higher-order frequency response and the transient response. Currently, direct tuning of the transient response to improve performance has to be done. One can tune the time domain response by looking into the influence of reset control parameters on the transient performance. Moreover, a link between frequency and transient response could be constructed if the impact of the control parameters is known on both.

V. Influence Control Parameters on Transient Response

The influence of different reset control parameters on the transient response is needed to gain insight into the tuning for transient performance. The following section gives an example of how this is explored in literature.

In [7], the influence of ω_l and γ is explored by simulating the step response of a CR CgLp architecture controlling a mass plant for a range of parameter values. In the CR CgLp structure, the reset condition can be approximated by (14).

$$\dot{e}(t)/\omega_l + e(t) = 0 \tag{14}$$

Therefore, ω_l determines the coefficients of $\dot{e}$ and e for the reset condition. This is the same behaviour as in Fig. 12 when the lead element was placed in front of the reset element. Higher values of ω_l will favour reset based on $e(t)$ since less lead is provided. For sufficiently large ω_l, the system behaves like a regular CgLp element since the lead provided is almost negligible. The effect of variations of γ and ω_l on the overshoot can be seen in Fig. 15. Here, ω_c is the intended bandwidth frequency of the system. Generally, decreasing γ, thereby increasing phase margin, leads to an almost linear decrease in overshoot. Decreasing ω_l also decreases overshoot, which is caused by the additional reset instances the lead provides. A no-overshoot response can be achieved when the right combination of γ and ω_l are selected.

However, decreasing ω_l too much could lead to excessive resetting action, negatively influencing settling time. In [7], a second simulation establishes the relationship between the control parameters and settling time. Fig. 16 shows that the settling time can be minimized while having a zero overshoot step response when $\omega_l \in [0.3\omega_c, 0.6\omega_c]$ and phase margin larger than 20°.

Based on these results, [7] provides rule of thumb values for the CR CgLp control parameters for mass plants to increase transient performance, see Table I. The method establishing these rule-of-thumb parameters can also be applied to mass-spring-damper plants and will result in similar suggested parameter values. The results are verified by implementing CR CgLp control in a precision motion system. The resulting step responses for different values of ω_l can be seen in Fig. 17. For this application, $\omega_l = 30Hz$

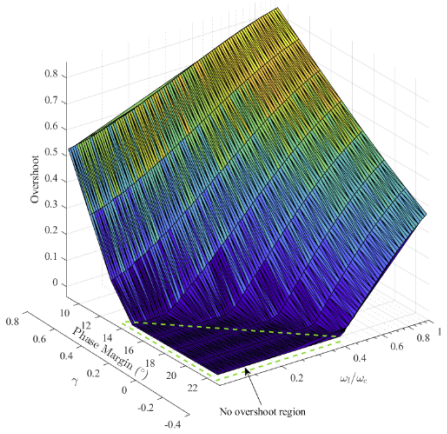

Fig. 15: Overshoot of a CR CgLp architecture to a step input for different γ and ω_l values [7].

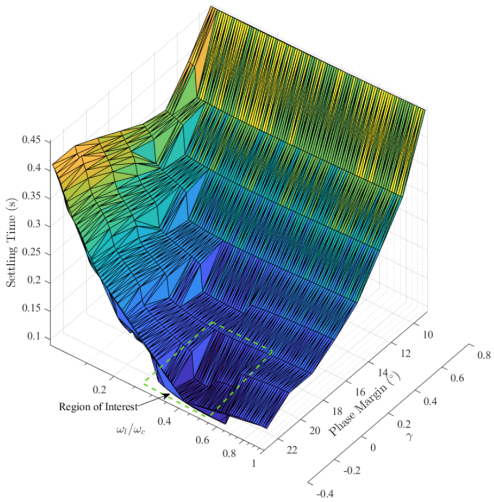

Fig. 16: Settling time of a CR CgLp architecture to a step input for different γ and ω_l values [7].

provides a no-overshoot response without deterioration of the settling time. Moreover, an example of the settling time suffering from the excessive reset action when $\omega_l = 10Hz$ can be seen.

These results show a simulation-based method for determining the influence of control parameters on the transient performance of a reset control system. Similar studies can be executed to find the influence of control parameters on the transient performance of a particular system. However, the simulations cannot provide insight into the exact relation

TABLE I: Rule of thumb values of control parameters CR CgLp controlling a mass plant [7].

Parameter	ω_r	PM	ω_l	ω_h	ω_f
Value	$[\omega_c, 1.5\omega_c]$	$[15°, 25°]$	$[0.3\omega_c, 0.6\omega_c]$	$20\omega_c$	$20\omega_c$

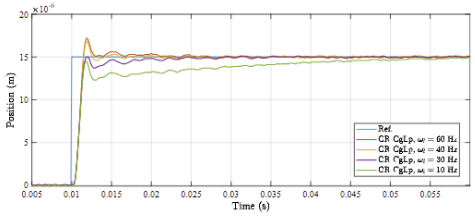

Fig. 17: Step response of CR CgLp controlling a precision motion system for different ω_l values [7].

between the control parameters and transient performance. An exact relation would provide a better understanding of the mechanics behind the increase/decrease of transient performance. This is especially relevant when a lead-reset system is considered since the additional reset instances are non-intuitive. Knowing how and when the controller will reset, makes way for better tuning of those systems and possibly the creation of improved reset control architectures to benefit from the decreased overshoot the lead can provide.

VI. Conclusion and Research Goal

Reset control is a method to overcome the inherent limitations of linear control. The phase margin of a system can be increased through the reduction of phase lag the reset provides. The transient performance benefits from the additional phase margin in decreasing overshoot. However, this is not the only way the transient performance can be improved through the application of reset control. It was shown that a reset controller could decrease overshoot and settling time even when it is compared to a linear system with an equal phase margin. Therefore, the transient performance is not only dependent on the phase margin of the system, and other reset characteristics are relevant.

Moreover, it was shown that the step response of a reset system depends on the sequence of control blocks. Different configurations of the same control elements cause different transient behavior while having the same first-order DF. Hence, the transient performance of a reset system cannot be entirely attributed to the first-order frequency response of the system. A clear and exact relation between the frequency response and the transient performance of a reset system is missing.

One can simultaneously increase steady-state and transient performance in linear control by only tuning in the frequency domain. Since the relation between frequency and time response of reset systems is not fully defined yet, the time and frequency domain tuning has to be done separately to ensure both steady-state and transient performance is sufficient.

The specific tuning for transient performance can be done by analyzing the influence of control parameters on the transient response. A simulation-based study in [7] showed how the CR CgLp architecture's control parameters

influence a system's transient response. From there, tuning guidelines are formed for a CR CgLp element combined with a linear PID, controlling a mass plant. Other systems could be investigated similarly to create tuning guidelines. However, this method of retrieving tuning guidelines relies on simulating a large range of parameter values. Gaining insight into the exact mechanics driving the transient response is hard this way.

Lastly, it was shown that a lead filter before a reset element in a CgLp changes the transient behavior by making the reset instances dependent on both the error and the derivative of the error. This structure shows great potential to increase both transient and steady-state performance. However, the lead can also cause excessive reset action, negatively affecting settling time. More insight is needed on how the lead-reset configurations improve the step response to better design the amount of lead provided and the control architecture.

In short, a systematic tuning method is needed to improve the transient performance of a reset system. If the transient response could be predicted based on the frequency response and the controller configuration, it could give way to new tuning and control strategies. More performance could be extracted by gaining insight into the dependence of damping on the exact controller sequence.

The goal of the thesis following this literature review is to develop a method of analyzing damping in reset control systems. This will be done by analytically solving the step response of a reset control system. The analytical expression provides a method of defining the damping of the transient response. It could be seen how the damping is affected when the controller sequence is changed.

REFERENCES

[1] Alfonso Baños and Antonio Barreiro. *Reset Control Systems*. Springer London, London, 2012.

[2] R H Munnig Schmidt, G Schitter, A Rankers, and J van Eijk. *The design of high performance mechatronics: high-tech functionality by multidisciplinary system integration (2nd revised edition)*, volume 2. IOS Press, Amsterdam, 2014.

[3] J. C. Clegg. A nonlinear integrator for servomechanisms. *Transactions of the American Institute of Electrical Engineers, Part II: Applications and Industry*, 77(1):41–42, 7 1958.

[4] Isaac Horowitz and Patrick Rosenbaum. Non-linear design for cost of feedback reduction in systems with large parameter uncertainty. *International Journal of Control*, 21(6):977–1001, 1975.

[5] Leroy Hazeleger, Marcel Heertjes, and Henk Nijmeijer. Second-order reset elements for stage control design. In *Proceedings of the American Control Conference*, volume 2016-July, pages 2643–2648. Institute of Electrical and Electronics Engineers Inc., 7 2016.

[6] Niranjan Saikumar, Rahul Kumar Sinha, and S. Hassan Hosseinnia. 'Constant in Gain Lead in Phase' Element-Application in Precision Motion Control. *IEEE/ASME Transactions on Mechatronics*, 24(3):1176–1185, 6 2019.

[7] Nima Karbasizadeh and S. Hassan HosseinNia. Continuous reset element: Transient and steady-state analysis for precision motion systems. *Control Engineering Practice*, 126:105232, sep 2022.

[8] Nima Karbasizadeh, Niranjan Saikumar, and S. Hassan HosseinNia. Fractional-order single state reset element. *Nonlinear Dynamics*, 2021.

[9] Duarte Valério, Niranjan Saikumar, Ali Ahmadi Dastjerdi, Nima Karbasizadeh, and S. Hassan HosseinNia. Reset control approximates complex order transfer functions. *Nonlinear Dynamics*, 97(4):2323–2337, 9 2019.

[10] Qian Chen, Yossi Chait, and CV Hollot. Analysis of reset control systems consisting of a fore and second-order loop. *J. Dyn. Sys., Meas., Control*, 123(2):279–283, 2001.

[11] O Beker, CV Hollot, Q Chen, and Y Chait. Stability of a reset control system under constant inputs. In *Proceedings of the 1999 American Control Conference (Cat. No. 99CH36251)*, volume 5, pages 3044–3045. IEEE, 1999.

[12] Yuhang Zheng, Y Chait, CV Hollot, M Steinbuch, and M Norg. Experimental demonstration of reset control design. *Control Engineering Practice*, 8(2):113–120, 2000.

[13] S Hassan HosseinNia, Inés Tejado, and Blas M Vinagre. Basic properties and stability of fractional-order reset control systems. In *2013 European Control Conference (ECC)*, pages 1687–1692. IEEE, 2013.

[14] S Hassan HosseinNia, Inés Tejado, and Blas M Vinagre. Fractional-order reset control: Application to a servomotor. *Mechatronics*, 23(7):781–788, 2013.

[15] S Hassan HosseinNia, Inés Tejado, Daniel Torres, Blas M Vinagre, and Vicente Feliu. A general form for reset control including fractional order dynamics. *IFAC Proceedings Volumes*, 47(3):2028–2033, 2014.

[16] Orhan Beker, C. V. Hollot, Yossi Chait, and Huaizhong Han. Fundamental properties of reset control systems. *Automatica*, 40(6):905–915, 6 2004.

[17] O. Beker, C. V. Hollot, and Y. Chait. Plant with integrator: An example of reset control overcoming limitations of linear feedback. *IEEE Transactions on Automatic Control*, 46(11):1797–1799, 11 2001.

[18] Daowei Wu, Guoxiao Guo, and Youyi Wang. Reset integral-derivative control for hdd servo systems. *IEEE Transactions on Control Systems Technology*, 15(1):161–167, 2006.

[19] Chengwei Cai. The Optimal Sequence for Reset Controllers. Technical report.

[20] P. W.J.M. Nuij, O. H. Bosgra, and M. Steinbuch. Higher-order sinusoidal input describing functions for the analysis of non-linear systems with harmonic responses. *Mechanical Systems and Signal Processing*, 20(8):1883–1904, 11 2006.

[21] Niranjan Saikumar, Kars Heinen, and S. Hassan HosseinNia. Loop-shaping for reset control systems: A higher-order sinusoidal-input describing functions approach. *Control Engineering Practice*, 111, 6 2021.

[22] Nima Karbasizadeh, Ali Ahmadi Dastjerdi, Niranjan Saikumar, Duarte Valerio, and S. Hassan HosseinNia. Benefiting from Linear Behaviour of a Nonlinear Reset-based Element at Certain Frequencies. 4 2020.

[23] Qian Chen. *Reset control systems: Stability, performance and application*. University of Massachusetts Amherst, 2000.

[24] Niranjan Saikumar, Duarte Valerio, and S. Hassan Hosseinnia. Complex order control for improved loop-shaping in precision positioning. In *Proceedings of the IEEE Conference on Decision and Control*, volume 2019-December, pages 7956–7962. Institute of Electrical and Electronics Engineers Inc., 12 2019.

[25] Yusuf Salman. TUNING A NOVEL RESET ELEMENT THROUGH DESCRIBING FUNCTION AND HOSIDF ANALYSIS. Technical report.

[26] Erdi Akyüz and Aky¨ Akyüz. Challenge the future Department of Precision and Microsystems Engineering Reset Control for Vibration Isolation. Technical report, 2018.

[27] Mark Ivens. Robust reset control using adaptive / iterative learning control. Technical report.

[28] Alfonso Baños, Sebastián Dormido, and Antonio Barreiro. Limit cycles analysis of reset control systems with reset band. *Nonlinear Analysis: Hybrid Systems*, 5(2):163–173, 5 2011.

[29] O. Beker, C. V. Hollot, and Y. Chait. Stability of limit-cycles in reset control systems. In *Proceedings of the American Control Conference*, volume 6, pages 4681–4682. Institute of Electrical and Electronics Engineers Inc., 2001.

[30] Nima Karbasizadeh, Ali Ahmadi Dastjerdi, Niranjan Saikumar, and S Hassan Hosseinnia. Band-Passing Nonlinearity in Reset Elements. Technical report.

[31] Guanglei Zhao, Dragan Nešić, Ying Tan, and Changchun Hua. Overcoming overshoot performance limitations of linear systems with reset control. *Automatica*, 101:27–35, 3 2019.

3

Objective

The literature review in Section 2 shows how reset control is currently used to improve the transient performance of motion control systems. The study provides a platform to define the literature gap that can be researched in the rest of this thesis.

3.1. Problem statement and research goal

The review has shown that reset control can be used beneficially to improve the transient response by providing additional damping compared to linear control. The damping in linear control is dependent on the phase margin and the controller sequence of the reset controller. Currently, the step response is calculated numerically to tune the transient response. However, this does not provide insight into how the damping is achieved. An analytical analysis of the transient response would provide a better understanding of the root of the additional damping and assist in developing new tuning guidelines. Therefore, the research goal is defined as follows:

Develop an analytical approach to analyze the damping of the transient response in reset control systems.

3.2. Research approach

Section 4 aims to achieve the proposed research goal. This is done by taking the following steps:

- Solve the step response and the states of reset control systems with mass plants analytically.
- Use the analytical solution of the reset control system to define the damping of the step response and use the definition to develop a method of analyzing the damping of a reset system.
- Validate the value of the method by analyzing the damping of a reset control system for different control sequences.

4

Damping Analysis of Transient Response in Reset Control Systems: an Analytical Approach

In this section, the main contribution of this thesis is provided in scientific paper form. First, the problems in analyzing the damping of reset systems are introduced. Secondly, background information is provided. Then the analytic solution of the transient response of reset control systems with mass plants is derived. Subsequently, two damping analysis methods are proposed using the analytical expressions. To show the significance of the proposed methods, the damping of a reset controller is analyzed for different controller sequences. Lastly, conclusions are presented and future work is proposed.

Note that the appendices being referenced in the paper are provided in the paper itself. Complementary to the content in the paper 3 appendices are provided at the end of this thesis. In Appendix A, a list of symbols and their description can be found. In Appendix B the derived step response expression is validated by comparing it to a simulated version of a reset controller. Finally, in Appendix C, Matlab functions are provided, which are created to aid in the calculation of the analytical response of a reset control system.

Damping Analysis of Transient Response in Reset Control Systems: an Analytical Approach

Mees Vanderbroeck*

Abstract— **The high-tech industry continuously pushes the boundaries of controller performance to achieve faster and more precise machines. Currently, linear control is the standard in the industry. These controllers suffer from the waterbed effect and Bode's phase/gain relation, which impose inherent limitations on the precision and robustness of the system. Reset control is a popular strategy to get around these limitations and improve performance. The damping in reset control systems is not only determined by the phase margin of the system but is also dependent on the exact controller element sequence. Currently, finding the optimal controller sequence is done through simulation of the step response. However, this fails to provide insight into the underlying cause of the additional damping achieved by specific controller configurations. This paper proposes an analytical approach to analyze the damping of the transient response reset control systems. The analytical analysis provides a better understanding of sequence-dependent damping and assists in controller design. First, the analytical expressions of the step response and states of the system are derived, which are used to define the system's energy. The step response and energy equations are used to characterize the damping in a reset control system. To show the value of the proposed method, the damping in a reset control system is assessed as an illustrative example. It is found that when a lead is in front of a reset element, the reset controller can provide more damping because it reduces the oscillatory content in the step response.**

Keywords: Nonlinear control, Reset control (RC), Transient response, Damping

I. Introduction

The high-tech industry continuously pushes the boundaries of controller performance to achieve faster and more precise machines. PID control is the current standard for controlling precision motion systems. With the use of loop-shaping and feed-forward techniques, high bandwidth, robust, and high precision control can be achieved. However, linear control suffers from the waterbed effect, and Bode's phase/gain relationship [1], [2]. These limit the level of robustness and precision achieved within linear control. By breaking Bode's phase/gain relationship and omitting the waterbed effect, higher bandwidth and precision can be achieved. Nonlinear control can offer an opportunity to satisfy the industry's increasing demands on controller performance [3]–[6].

Reset control is a nonlinear control technique popularised due to its compatibility with PID control and loop-shaping techniques. Reset control involves resetting one or multiple states of a controller when a reset condition is satisfied. The first reset control element was a resetting integrator introduced by Clegg [7]. This reset element could reduce the phase lag of the linear integrator significantly. Since then, many other reset elements have been introduced and implemented [8]–[13]. In general, reset elements can reduce the phase lag of a control system compared to its linear counterpart without compromising other aspects of the controller. In literature, it is shown that reset control can significantly improve controller performance in the frequency domain and steady-state response [14]–[22].

The advantages of reset controllers can also be seen in improved transient performance with the reduction and prevention of overshoot [8], [20], [21], [23]. In linear control of motion systems, a reduction in overshoot can be attributed to an increase in phase margin. However, [24] shows that the sequence of the control elements can change the overshoot of a reset control system (RCS) independent of the phase margin. In [24] and [11], it is shown that placing a lead before a reset element can reduce overshoot compared to when the lead is after the reset element. Currently, the step response is simulated to find the optimal controller configuration for transient performance. However, this fails to provide insight into the underlying cause of the extra damping achieved by specific control element sequences. Suppose the damping of the step response could be analyzed analytically, independently of the phase margin. In that case, the origin of the additional damping could be better understood and used to improve the design of reset controllers to enhance transient performance.

The contribution of this paper is to develop an analytical approach to analyze the damping of the transient response in reset control systems. This approach relies on deriving an analytical expression of the step response and the system's states. With these expressions, the dependence of damping on the controller sequence can be determined. To show the merit of the damping analysis, the step response of a reset controller is analyzed for different controller sequences as an illustrative example. The rest of the paper will be structured as follows. In Section II, background knowledge on reset control is provided. Section III contains the analytical derivation of the step response, its derivatives, and the states of a general reset control system. The damping analysis methods of base linear stable reset control systems are proposed in Section IV. Section V provides an illustrative example of the proposed methods. Lastly, conclusions and future work are discussed in section VI.

* Department of Precision and Microsystem Engineering, Delft University of Technology, Delft, The Netherlands

II. Preliminaries

A. Definition general reset controller

Reset control systems can be written as (1).

$$\Sigma_R := \begin{cases} \dot{x}_r = A_r x_r(t) + B_r e(t), & \text{if} \quad e(t) \neq 0 \\ x_r(t^+) = A_\rho x_r(t), & \text{if} \quad e(t) = 0 \\ u(t) = C_r x_r(t) + D_r e(t) \end{cases} \tag{1}$$

Matrices A_r, B_r, C_r, D_r describe the state-space representation of the Base Linear System (BLS) of the reset system. The BLS is equivalent to the reset system without resetting action. Matrix A_ρ determines the amount of reset for each state when the reset condition is met. $x_r(t)$, $e(t)$, and $u(t)$ describe the reset controller states, controller input, and controller output, respectively.

B. Relevant reset elements

1) Clegg integrator: The Clegg Integrator (CI) was the first reset element introduced in [7]. Based on describing function analysis, a reduction of $52°$ phase lag can be achieved by applying reset to a linear integrator. The state-space representation of a CI can be written to the form in (1), where:

$$A_r = 0, B_r = 1, C_r = 1, D_r = 0, A_\rho = 0 \tag{2}$$

2) (Generalized) First/Second Order Reset Element: As an extension of the CI, the First Order Reset Element (FORE) was introduced in [8]. FORE is a first-order low-pass filter with resetting action. It provides more design freedom than the CI by changing the filter's corner frequency ω_r. The conventional FORE in [8] fully resets when the reset condition is met. The generalized FORE (GFORE), introduced in [25], also allows for a partial reset of the FORE. The amount of reset is defined as γ. Note that the actual corner frequency of the reset filter is different from ω_r. The actual corner frequency shifts for different values of γ. The frequency shift can be accounted for by using $\omega_{r\alpha_s} = \omega_r/\alpha_s$ instead. Here α_s is a correction factor whose value depends on the amount of reset according to [10]. The state-space representation of GFORE can be written to the form in (1), where:

$$A_r = -\omega_r, B_r = \omega_r, C_r = 1, D_r = 0, A_\rho = \gamma \tag{3}$$

The reset equivalent of a second-order low-pass filter is called a Second Order Reset Element (SORE) and was introduced in [9]. The additional control parameter β_r can be used to change the damping of the element. The generalized SORE (GSORE) also allows partial reset determined by γ_1 and γ_2. Both parameters individually determine the amount of reset of each separate controller state. A state-space representation of GSORE can be written to the form in (1), where:

$$\begin{gathered} A_r = \begin{bmatrix} 0 & 1 \\ -\omega_r^2 & -2\beta_r\omega_r \end{bmatrix}, B_r = \begin{bmatrix} 0 \\ \omega_r^2 \end{bmatrix}, \\ C_r = \begin{bmatrix} 1 & 0 \end{bmatrix}, D_r = [0], A_\rho = \begin{bmatrix} \gamma_1 & 0 \\ 0 & \gamma_2 \end{bmatrix} \end{gathered} \tag{4}$$

In contrast to linear control, the exact state-space representation of a reset system does influence the output of the system in nonlinear control [26]. In other words, the output depends on the exact configuration of the control elements because the superposition principle does not apply [27]. The correct state-space representation should be used to describe the actual reset control system.

Both GFORE and GSORE can be described in transfer function form:

$$GFORE(s) = \frac{1}{s/\omega_r + 1}^{\gamma} \tag{5}$$

$$GSORE(s) = \frac{1}{(s/\omega_r)^2 + (2s\beta_r/\omega_r) + 1}^{\gamma_1,\gamma_2} \tag{6}$$

The arrow crossing the equation shows that the element is a reset element with γ_1 and γ_2 defining the amount of reset of each state.

3) Constant in Gain Lead in Phase: The Constant in gain Lead in phase (CgLp) element was introduced in [10]. The element can create phase lead while the gain remains constant by using the difference in phase shift of a linear and a reset element.

A CgLp element combines a reset lag filter $R(s)$ with a linear lead filter $L(s)$ of equal order. The reset lag filter can be a GFORE or GSORE. These filters can be described in transfer function form:

$$R(s) = \frac{1}{s/\omega_{r\alpha_s} + 1}^{\gamma} \quad \text{or} \quad \frac{1}{(s/\omega_{r\alpha_s})^2 + (2s\beta_r/\omega_{r\alpha_s}) + 1}^{\gamma} \tag{7}$$

and

$$L(s) = \frac{s/\omega_r + 1}{s/\omega_f + 1} \quad \text{or} \quad \frac{(s/\omega_r)^2 + (2s\beta_r/\omega_r) + 1}{(s/\omega_f)^2 + (2s/\omega_f) + 1} \tag{8}$$

ω_r and ω_f are the lead filter's corner frequency and termination frequency, respectively. $\omega_{r\alpha_s} = \omega_r/\alpha_s$ is the corner frequency correction of the reset element to match the corner frequency ω_r of the lead filter. For frequencies between ω_r and ω_f, the CgLp provides phase lead with unity gain, as seen in Fig. 1. State-space matrices of a CgLp element consisting of a GFORE are as follows:

$$\begin{gathered} A_r = \begin{bmatrix} -\omega_{r\alpha_s} & 0 \\ -\omega_f & \omega_f \end{bmatrix}, B_r = \begin{bmatrix} \omega_{r\alpha_s} \\ 0 \end{bmatrix}, \\ C_r = \begin{bmatrix} \frac{\omega_f}{\omega_r} & (1 - \frac{\omega_f}{\omega_r}) \end{bmatrix}, D_r = [0], A_\rho = \begin{bmatrix} \gamma & 0 \\ 0 & 1 \end{bmatrix} \end{gathered} \tag{9}$$

Note that this state-space representation describes a CgLp where the lead element is after the reset element. The

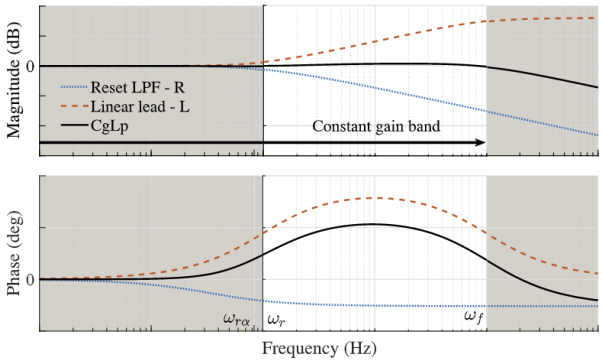

Fig. 1: First-order describing function of a CgLp element [10].

state-space realization should be changed when the order is switched.

C. Describing functions

Loop shaping techniques are the industry standard for tuning controllers. This technique is based on the frequency response of the system. Unfortunately, the frequency response of a nonlinear system cannot be captured entirely by a single frequency domain function. The frequency response function of nonlinear systems can be approximated with the Describing Function (DF) [28]. The DF is primarily used in the design of reset control systems. However, this approximation only considers the first harmonic of the Fourier series. Therefore, only considering the DF may be an inaccurate approximation of the frequency domain response of a nonlinear system. To consider the effect of higher-order harmonics, the Higher Order Sinusoidal Input Describing Functions (HOSIDFs) of the nonlinear system introduced in [25] can be calculated. The HOSIDFs of a reset element described in (1) can be found by using (10) introduced in [29].

$$G_n(j\omega) = \begin{cases} C_r(j\omega I - A_r)^{-1}(I + j\Theta_\rho(\omega))B_r + D_r & n = 1 \\ C_r(nj\omega I - A_r)^{-1}(I + j\Theta_\rho(\omega))B_r & \text{odd } n \geq 2 \\ 0 & \text{even } n \geq 2 \end{cases} \tag{10}$$

Where,

$$\begin{aligned} \Theta_\rho(\omega) &= \frac{2\omega^2}{\pi}\Delta(\omega)(\Gamma(\omega) - \Lambda^{-1}) \\ \Gamma(\omega) &= \Delta_\rho(\omega)^{-1}A_\rho\Delta(\omega)\Lambda(\omega)^{-1} \\ \Delta_\rho(\omega) &= I + A_\rho e^{\frac{A_r\pi}{\omega}} \\ \Delta(\omega) &= I + e^{\frac{A_r\pi}{\omega}} \\ \Lambda(\omega) &= \omega^2 I + A_r \end{aligned} \tag{11}$$

In general, the loop-shaping of reset control systems is based on the first-order DF. Furthermore, the system is tuned to reduce the magnitude of the HOSIDFs to make the approximation of the frequency response by DF as representative as possible.

III. Analytical Derivation Step Response of Reset Control System with Mass Plants

Consider the general Single-Input Single-Output (SISO) reset control system with a mass plant $P(s) = \frac{1}{ms^2}$ in Fig. 2. The closed-loop system consists of two linear controllers $C_1(s)$ and $C_2(s)$. These are placed before and after the reset control element Σ_R. The shaping filter $SF(s)$ output defines the reset condition of Σ_R.

The system can mathematically be described by the system of equations in (12)-(21). Here $\{A_{c_1}, B_{c_1}, C_{c_1}, D_{c_1}\}$ and $\{A_{c_2p}, B_{c_2p}, C_{c_2p}\}$ are the minimal realizations of $C_1(s)$ and $C_2(s)P(s)$ respectively. Likewise, $\{A_r, B_r, C_r, D_r, A_\rho\}$ is the minimal realization of the reset element Σ_R as shown in (1). $x_{c_1} \in \mathbb{R}^{n_1}$, $x_r \in \mathbb{R}^{n_r}$, and $x_{c_2p} \in \mathbb{R}^{n_2}$ are the states of the first linear controller, the reset element, and the linear elements after the reset block. A_ρ is the reset matrix of the reset element. Finally, $\{A_{sf}, B_{sf}, C_{sf}, D_{sf}\}$ is the minimal realization of the shaping filter with state $x_{sf} \in \mathbb{R}^{n_{sf}}$. In this analysis, only physical systems are considered. Therefore, the system can be assumed to be strictly proper, and output $y(t)$ only depends on states $x_{c_2p}(t)$.

$$\begin{cases} \dot{x}_{c_1}(t) &= A_{c_1}x_{c_1}(t) + B_{c_1}e(t) & (12) \\ u_{c_1}(t) &= C_{c_1}x_{c_1}(t) + D_{c_1}e(t) & (13) \\ \dot{x}_{sf}(t) &= A_{sf}x_{sf}(t) + B_{sf}u_{c_1}(t) & (14) \\ u_{sf}(t) &= C_{sf}x_{sf}(t) + D_{sf}u_{c_1}(t) & (15) \\ \dot{x}_r(t) &= A_r x_r(t) + B_r u_{c_1}(t), \quad u_{sf}(t) \neq 0 & (16) \\ x_r(t^+) &= A_\rho x_r(t), \quad u_{sf}(t) = 0 & (17) \\ u_r(t) &= C_r x_r(t) + D_r u_{c_1}(t) & (18) \\ \dot{x}_{c_2p}(t) &= A_{c_2p}x_{c_2p}(t) + B_{c_2p}u_r(t) & (19) \\ y(t) &= C_{c_2p}x_{c_2p}(t) & (20) \\ e(t) &= r(t) - y(t) & (21) \end{cases}$$

The closed-loop state-space representation of the complete system can be written as follows:

$$\begin{cases} \dot{x}(t) = A_{cl}x(t) + B_{cl}r(t), & \text{if} \quad u_{sf}(t) \neq 0 \\ x(t^+) = \hat{A}_\rho x(t), & \text{if} \quad u_{sf}(t) = 0 \\ y(t) = C_{cl}x(t) \\ u_{sf}(t) = C_{rline}x(t) + D_{rline}r(t) \end{cases} \tag{22}$$

Where,

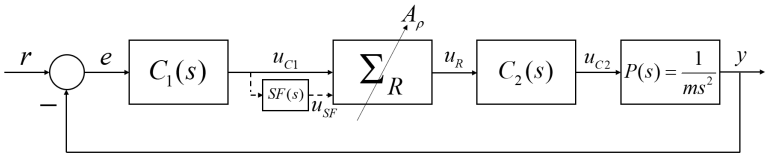

Fig. 2: General SISO reset control system with a mass plant.

$$
\begin{aligned}
x(t) &= \begin{bmatrix} x_r \\ x_{c_1} \\ x_{sf} \\ x_{c_2p} \end{bmatrix}, x(t) \in \mathbb{R}^n \\
A_{cl} &= \mathbb{R}^{n\times n}, B_{cl} = \mathbb{R}^n \\
C_{cl} &= \begin{bmatrix} 0^{n-n_2} & C_{c_2p} \end{bmatrix}, \\
\hat{A}_\rho &= \begin{bmatrix} A_\rho & 0 \\ 0 & I^{(n-n_r)\times(n-n_r)} \end{bmatrix} \\
C_{rline} &= \begin{bmatrix} 0^{n_r} \\ D_{sf}C_{c_1} \\ C_{sf} \\ -D_{sf}D_{c_1}C_{c_2p} \end{bmatrix}^T, \\
D_{rline} &= D_{sf}D_{c_1}
\end{aligned} \tag{23}
$$

The entries of A_{cl} and B_{cl} depend on the state-space matrices of the individual control elements. The expressions of the entries of A_{cl} and B_{cl} can be found in Appendix A.

A. Energy and Power of mass plant

In motion control systems, damping can be defined as the dissipation of the plant's energy. As a result, oscillations are suppressed, and the response is slowed. The energy of the system in Fig. 2 only depends on the kinetic energy of the plant since it controls a single mass plant.

$$E(t) = \frac{1}{2}m\dot{y}(t)^2 \tag{24}$$

The only way the plant's energy can change is when the controller applies power to the plant since no other forces are considered. The power delivered by the controller can be described by:

$$P(t) = \frac{d}{dt}E(t) = m\ddot{y}(t)\dot{y}(t) \tag{25}$$

When the controller applies negative power to the plant, the sign of the acceleration and the velocity terms have to be opposite. In short, the controller provides damping to the system when the power is negative. Therefore, the damping of a mass plant system can be analyzed by looking at the acceleration and velocity response. When the acceleration and velocity response could be described analytically, the damping would also be described analytically.

B. Analytical derivation of solution of RCS with mass plants

In this section, the analytical expressions of the step response and its derivatives are derived for the reset control system in Fig. 2. It needs to be proven that the system can be transformed into a zero-input/unforced system when the reference is constant to find the expressions. Then the solution of the step response of the reset control system can be found by considering the homogeneous solution of the base linear system to multiple linked initial value problems. The initial state of the new initial value problem after any reset is the last state just before the reset, which has been reset. Furthermore, by decomposing the system matrix A_{cl}, the step response can be written as a linear combination of sine, cosine, and exponential terms, which depend on the eigenvalues and eigenvectors of the system matrix. Finally, the step response expression can be differentiated to retrieve an expression for the velocity and acceleration response.

This paper considers the damping of the transient response of reset control systems. Therefore, a step input is considered the system's input for the remainder of this paper. This section provides an analytical solution to the step response of the reset control system. The solution can then be used to analyze the damping of the step response.

First, let the set I of all reset instances be defined by (26).

$$I = \{t_i | u_{sf}(t_i) = 0, t_i = \langle t_{i-1}, t_{i+1} \rangle, i = 0, 1, 2, ...\} \tag{26}$$

Additionally, consider $t_0 = 0$ as the step instance of the reference. During and after the step instance, the reference will be constant $r(t) = r_0, t \geq t_0$. t_0 is also the starting point of the analysis. Since only physical systems with a mass plant are considered, we can assume the following:

Assumption 1. *$C_2P(s)$ contains at least one integrator.*

This assumption leads to the following Lemma, as introduced in [30].

Lemma 1. *Consider the response of the closed-loop RCS in (22) for a constant reference input $r(t) = r_0$. Suppose Assumption 1 holds. Then there exists a $x_{c_2p0} \in \mathbb{R}^{n_2}$ for which $A_{c_2p}x_{c_2p0} = 0$, and $C_{c_2p}x_{c_2p0} = r_0$.*

Proof: If $C_2P(s)$ contains an internal model of $r(t) = r_0$ there exits a $x_{c_2p0} \in \mathbb{R}^{n_2}$ for which $A_{c_2p}x_{c_2p0} = 0$, and $C_{c_2p}x_{c_2p0} = r_0$. Therefore, such an x_{c_2p0} exists when $C_2P(s)$ contains at least one integrator since $\mathcal{L}\{r_0\} = \frac{r_0}{s}$. ■

Now define system (27), which is a zero-input version of system (22). In this system, the step height r_0 is only found in the system's output $y(t)$.

$$\begin{cases} \dot{\hat{x}} = A_{cl}\hat{x}(t), & \text{if} \quad u_{sf}(t) \neq 0 \\ \hat{x}(t^+) = \hat{A}_\rho \hat{x}(t), & \text{if} \quad u_{sf}(t) = 0 \\ y(t) = C_{cl}\hat{x}(t) + r_0 \\ u_{sf}(t) = C_{rline}\hat{x}(t) \end{cases} \tag{27}$$

Then the existence of x_{c_2p0} can be used to prove Lemma 2.

Lemma 2. *Suppose Assumption 1 holds. Consider a constant reference $r(t) = r_0$. The system (22) and (27) are equivalent under the state transformation $\hat{x}(t) = x(t) - x_0$, where $x_0 = \begin{bmatrix} 0^{n-n_2} x_{c_2p0} \end{bmatrix}^T$.*

Proof: First, substitute the state transformation back into system (27):

$$\begin{cases} \dot{x} - \dot{x}_0 = A_{cl}x(t) - A_{cl}x_0, & \text{if}\, u_{sf}(t) \neq 0 \\ x(t^+) - x_0 = \hat{A}_\rho x(t) - \hat{A}_\rho x_0, & \text{if}\, u_{sf}(t) = 0 \\ y(t) = C_{cl}x(t) - C_{cl}x_0 + r_0 \\ u_{sf}(t) = C_{rline}x(t) - C_{rline}x_0 \end{cases} \tag{28}$$

Now use the fact that $\dot{x}_0 = 0$, $\hat{A}_\rho x_0 = x_0$, the element expressions of $A_{cl}, B_{cl}, C_{cl}, C_{rline}$, and D_{rline} which can be found in (23) and Appendix A. Lastly, use $A_{c_2p}x_{c_2p0} = 0$ and $C_{c_2p}x_{c_2p0} = r_0$ from Lemma 1, to find that (27) is equivalent to (22). ■

A more detailed proof can be found in Appendix B.

Remark 1. Since $C_2P(s)$ contains at least one integrator, the transformation state x_0 can be written as follows:

$$x_0 = \begin{bmatrix} 0^{n-n_2} & d_1 & d_2 & \cdots & d_{n_2-1} & 1 \end{bmatrix}^T r_0 \tag{29}$$

Coefficients d_j for $j = 1, 2, \cdots, n_2 - 1$ correspond to the denominator coefficients in the form of $C_2P(s)$ in (30).

$$C_2P(s) = \frac{c_{n_2-1}s^{n_2-1} + \cdots + c_1 s + c_0}{s^{n_2} + d_{n_2-1}s^{n_2-1} + \cdots + d_1 s} \tag{30}$$

Remark 2. From (27) and (26) it can be concluded that between reset instances t_i and t_{i+1} the system behaves like the BLS:

$$\dot{\hat{x}}(t) = A_{cl}\hat{x}(t), \qquad t \in \langle t_i, t_{i+1}] \tag{31}$$

Theorem 1. *Consider the RCS in (22) and its transformed equivalent in (27). Suppose Assumption 1 holds and $r(t) = r_0$. Then the system response can be expressed as:*

$$\hat{x}(t) = e^{A_{cl}(t-t_i)}\hat{x}(t_i) = \Phi(t - t_i)\hat{x}(t_i), \qquad t \in \langle t_i, t_{i+1}] \tag{32}$$

Here, $\Phi(t)$ is called the state-transition matrix.

Proof: Lemma 2 shows that the original system in (22) is equivalent to the zero-input system shown in (27). The solution of the base linear version of the zero-input system is:

$$\hat{x} = e^{A_{cl}t}\hat{x}(0) \tag{33}$$

Following Remark 2, the system behaves like the BLS when $t \notin I$. Therefore, the response between two reset instances will be a linear initial value problem, where the states at the last reset instance are the initial states, as expressed in (32). ■

Assumption 2. *A_{cl} is diagonalizable with n distinct eigenvalues.*

Lemma 3. *Suppose Assumption 2 holds. Then the response of the RCS depends on the eigenvalues and eigenvectors, reset instances, and the states at those resets. The entries of the transition matrix are:*

$$\Phi_{kl}(t - t_i) = \sum_{j=1}^{n} a_{kj}b_{jl}e^{\lambda_j(t-t_i)} \tag{34}$$

in which $a_{kj} = V_{kj}$, $b_{jl} = (V^{-1})_{jl}$, $\lambda_j = \Lambda_{jj}$. Here V contains the eigenvectors and Λ the eigenvalues of A_{cl}.

Proof: If A_{cl} is diagonalizable, it can be decomposed in $A_{cl} = V\Lambda V^{-1}$. Therefore, the transition matrix can expressed as $\Phi(t - t_i) = Ve^{A_{cl}(t-t_i)}V^{-1}$. Which leads to the expression in (34). Combining (32) and (34) shows the dependence on the eigenvalues and eigenvectors of A_{cl}, the reset instances, and the states at the reset instances. ■

Lemma 4. *Consider Assumption 2 holds. Moreover, consider λ_h and λ_m to be a complex conjugate pair of eigenvalues of A_{cl}, such that $\lambda_h = \overline{\lambda_m}$. Then,*

$$a_{kh}b_{hl} = \overline{a_{km}b_{ml}} = \sigma_{kl,h} + \tau_{kl,h}i \tag{35}$$

In which, $\sigma kl, h$ is the real part of $a_{kh}b_{hl}$ and $\underline{a_{km}b_{ml}}$. Moreover, $\tau_{kl,h}$ is the imaginary part of $a_{kh}b_{hl}$ and $\underline{a_{km}b_{ml}}$.

Proof: System matrix A_{cl} can be written as $A_{cl} = V\Lambda V^{-1}$ since it is assumed to be diagonalizable in Assumption 2. A_{cl} is considered to be real in (23). Therefore, all imaginary terms should cancel each other for A_{cl} to be real:

$$\Im(\sum_{j=1}^{n} a_{kj}b_{jl}\lambda_j) = 0 \tag{36}$$

Then, (35) needs to hold if λ_h and λ_m are a complex conjugate pair of eigenvalues. Hence, the claim is proven. ■

Lemma 5. *Consider the RCS in (27) for a constant step reference r_0. Suppose Assumptions 1 and 2 hold. Then the states of the RCS can be described by:*

$$\hat{x}_k(t) = \sum_{l=1}^{n} \Phi_{kl}(t - t_i)\hat{x}_l(t_i), \qquad t \in \langle t_i, t_{i+1}] \tag{37}$$

Where, the expression of state-transition matrix entry Φ_{kl} is:

$$\begin{aligned} \Phi_{kl}(t - t_i) = \sum_{j=1}^{n_{pair}} & 2e^{\alpha_j(t-t_i)}[\sigma_{kl,j}\cos(\beta_j(t - t_i)) \\ & - \tau_{kl,j}\sin(\beta_j(t - t_i))] \\ & + \sum_{q=n_{imag}+1}^{n} a_{kq}b_{ql}e^{\lambda_q(t-t_i)} \end{aligned} \tag{38}$$

In which, $\lambda_{2j-1} = \overline{\lambda_{2j}} = \alpha_j + \beta_j i$, $a_{n(2j-1)}b_{(2j-1)l} = \overline{a_{n(2j)}b_{(2j)l}} = \sigma_{nl,j} + \tau_{nl,j}i$, and $\Im(\lambda_q) = 0$. Finally, n_{pair} is the number of complex conjugate pairs of eigenvalues of A_{cl} such that $n_{imag} = 2n_{pair}$ and $n_{real} = n - 2n_{pair}$.

Proof: The eigenvalues of the closed-loop system matrix A_{cl} can either be real or be part of a complex conjugate pair of eigenvalues. Consider the complex conjugate pair of eigenvalues λ_h and λ_m, $\lambda_h = \overline{\lambda_m} = \alpha + \beta i$. Then the terms in (34) that are linked to this pair of eigenvalues can be expressed by (39) when Lemma 4 is applied.

$$\begin{aligned} &a_{kh}b_{hl}e^{\lambda_h(t-t_i)} + a_{km}b_{ml}e^{\lambda_m(t-t_i)} \\ &\quad=\sigma_{kl,h}e^{\alpha(t-t_i)}\big(e^{\beta(t-t_i)i} + e^{-\beta(t-t_i)i}\big) \\ &\qquad+ \tau_{kl,h}e^{\alpha(t-t_i)}\big(e^{\beta(t-t_i)i} - e^{-\beta(t-t_i)i}\big) \end{aligned} \tag{39}$$

Now Euler's formula is used to rewrite (39) to:

$$\begin{aligned} &a_{kh}b_{hl}e^{\lambda_h(t-t_i)} + a_{km}b_{ml}e^{\lambda_m(t-t_i)} \\ &\quad=2\sigma_{kl,h}e^{\alpha(t-t_i)}\cos\left(\beta(t-t_i)\right) \\ &\qquad- 2\tau_{kl,h}e^{\alpha(t-t_i)}\sin(\beta(t-t_i)) \end{aligned} \tag{40}$$

The substitution of (40) into (34) for every complex conjugate pair of eigenvalues results in (38). Therefore, the states of the RCS (27) can be described by (37). ■

Without loss of generality, the following assumption can be made:

Assumption 3. *The state-space representation of $C_2P(s)$ is in observable canonical form, such that $C_{cl} = \begin{bmatrix}0^{n-1} & 1\end{bmatrix}$.*

Theorem 2. *Consider the RCS in (27) for a constant step reference r_0. Suppose Assumptions 1-3 hold. Then the step response of the system is defined as:*

$$y(t) = r_0 + \sum_{l=1}^{n} \Phi_{nl}(t-t_i)\hat{x}_l(t_i), \qquad t \in \langle t_i, t_{i+1}] \tag{41}$$

The Φ_{nl} is the last row of the state-transition matrix.

Proof: Since Assumption 3 holds, the step response will be the sum of step height r_0 and the value of state $\hat{x}_n(t)$. Using Lemma 5 to rewrite $\hat{x}_n(t)$ gives (41). ■

Corollary 1. *Consider the RCS in (27) for a constant step reference r_0. Suppose Assumptions 1-3 hold. Then the velocity response of the system is defined as:*

$$\dot{y}(t) = \sum_{l=1}^{n} \dot{\Phi}_{nl}(t-t_i)\hat{x}_l(t_i), \qquad t \in \langle t_i, t_{i+1}] \tag{42}$$

Where the time derivative of the state-transition matrix entry $\dot{\Phi}_{nl}$ is:

$$\begin{aligned} \dot{\Phi}_{nl}(t-t_i) = &\sum_{j=1}^{n_{pair}} 2e^{\alpha_j(t-t_i)} \\ &\big[(\alpha_j\sigma_{nl,j} - \beta_j\tau_{nl,j})\cos(\beta_j(t-t_i)) \\ &- (\beta_j\sigma_{nl,j} + \alpha_j\tau_{nl,j})\sin(\beta_j(t-t_i))\big] \\ &+ \sum_{q=n_{imag}+1}^{n} \lambda_q a_{nq}b_{ql}e^{\lambda_q(t-t_i)} \end{aligned} \tag{43}$$

Proof: The derivative of the state-transition matrix entries can be split into cosine, sine, and exponential terms. The derivative of the cosine terms is:

$$\begin{aligned} &\frac{d}{dt}\big(2\sigma_{nl,j}e^{\alpha_j(t-t_i)}\cos\left(\beta_j(t-t_i)\right)\big) = \\ &\qquad 2\sigma_{nl,j}\alpha_j e^{\alpha_j(t-t_i)}\cos\left(\beta_j(t-t_i)\right) \\ &\qquad -2\sigma_{nl,j}\beta_j e^{\alpha_j(t-t_i)}\sin\left(\beta_j(t-t_i)\right) \end{aligned} \tag{44}$$

Similarly, the derivative of the sine terms is:

$$\begin{aligned} &\frac{d}{dt}\big(-2\tau_{nl,j}e^{\alpha_j(t-t_i)}\sin\left(\beta_j(t-t_i)\right)\big) = \\ &\qquad -2\tau_{nl,j}\alpha_j e^{\alpha_j(t-t_i)}\sin\left(\beta_j(t-t_i)\right) \\ &\qquad -2\tau_{nl,j}\beta_j e^{\alpha_j(t-t_i)}\cos\left(\beta_j(t-t_i)\right) \end{aligned} \tag{45}$$

Finally, the derivative of the terms corresponding to the real eigenvalues:

$$\frac{d}{dt}\big(a_{nq}b_{ql}e^{\lambda_q(t-t_i)}\big) = \lambda_q a_{nq}b_{ql}e^{\lambda_q(t-t_i)} \tag{46}$$

Combining the sinusoidal and exponential terms in (44)-(46) yields the derivative of the state-transition entries in (43). ■

Corollary 2. *Consider the RCS in (27) for a constant step reference r_0. Suppose Assumptions 1-3 hold. Then the acceleration response of the system is defined as:*

$$\ddot{y}(t) = \sum_{l=1}^{n} \ddot{\Phi}_{nl}(t-t_i)\hat{x}_l(t_i), \qquad t \in \langle t_i, t_{i+1}] \tag{47}$$

Where the second time derivative of the state-transition matrix entry $\ddot{\Phi}_{nl}$ is:

$$\begin{aligned} \ddot{\Phi}_{nl}(t-t_i) = &\sum_{j=1}^{n_{pair}} 2e^{\alpha_j(t-t_i)} \\ &\big[(\alpha_j^2\sigma_{nl,j} - 2\alpha_j\beta_j\tau_{nl,j} - \beta_j^2\sigma_{nl,j})\cos(\beta_j(t-t_i)) \\ &- (\alpha_j^2\tau_{nl,j} + 2\alpha_j\beta_j\sigma_{nl,j} - \beta_j^2\tau_{nl,j})\sin(\beta_j(t-t_i))\big] \\ &+ \sum_{q=n_{imag}+1}^{n} \lambda_q^2 a_{nq}b_{ql}e^{\lambda_q(t-t_i)} \end{aligned} \tag{48}$$

Proof: The second derivative of the state-transition matrix entries can again be split into cosine, sine, and exponential terms, similar to the proof of Corollary 1. The derivative of the cosine terms in the entry of the velocity state-transition matrix is:

$$\begin{aligned} &\frac{d}{dt}\big(2(\alpha_j\sigma_{nl,j} - \beta_j\tau_{nl,j})e^{\alpha_j(t-t_i)}\cos(\beta_j(t-t_i))\big) = \\ &\quad 2\alpha_j(\alpha_j\sigma_{nl,j} - \beta_j\tau_{nl,j})e^{\alpha_j(t-t_i)}\cos(\beta_j(t-t_i)) \\ &\quad -2\beta_j(\alpha_j\sigma_{nl,j} - \beta_j\tau_{nl,j})e^{\alpha_j(t-t_i)}\sin(\beta_j(t-t_i)) \end{aligned} \tag{49}$$

Similarly, the derivative of the sine terms is:

$$\begin{aligned} &\frac{d}{dt}\big(-2(\beta_j\sigma_{nl,j} + \alpha_j\tau_{nl,j})e^{\alpha_j(t-t_i)}\sin(\beta_j(t-t_i))\big) = \\ &\quad -2\alpha_j(\beta_j\sigma_{nl,j} + \alpha_j\tau_{nl,j})e^{\alpha_j(t-t_i)}\sin(\beta_j(t-t_i)) \\ &\quad -2\beta_j(\beta_j\sigma_{nl,j} + \alpha_j\tau_{nl,j})e^{\alpha_j(t-t_i)}\cos(\beta_j(t-t_i)) \end{aligned} \tag{50}$$

Finally, the derivative of the terms corresponding to the real eigenvalues:

$$\frac{d}{dt}\left(\lambda_q a_{nq} b_{ql} e^{\lambda_q (t-t_i)}\right) = \lambda_q^2 a_{nq} b_{ql} e^{\lambda_q (t-t_i)} \tag{51}$$

Combining the sinusoidal and exponential terms in (49)-(51) yields the second derivative of the state-transition entries in (48). ■

Now (42) and (47) can be used to express the energy and power of the plant analytically. The energy and power expressions can be used to analyze the damping in the step response for all reset control systems described by Fig. 2 as long as Assumptions 1-3 are valid. Moreover, the analytical expression of the step response itself can be used to see the effect of different controllers on the damping of the response.

IV. Damping Analysis of reset control systems with stable BLS

In this section, the analytical expressions introduced in Section III are used to analyze the damping of base linear stable reset control systems in Fig. 2. For the BLS to be stable, the eigenvalues of the system matrix A_{cl} in (23) are all required to have a negative real part. Therefore, $\alpha_j < 0$ and $\lambda_{Rh} < 0$ for all positive integers j and h in (52).

$$\lambda = \begin{bmatrix} \alpha_1 + \beta_1 i \\ \alpha_1 - \beta_1 i \\ \vdots \\ \alpha_{n_{pair}} + \beta_{n_{pair}} i \\ \alpha_{n_{pair}} - \beta_{n_{pair}} i \\ \lambda_{R1} \\ \vdots \\ \lambda_{Rn_{real}} \end{bmatrix} \tag{52}$$

Note that λ_{Rh} is the $q = h + n_{imag}$-th eigenvalue of the system. Theorem 2 can be used to express the step response of the RCS analytically in (53). Note that the coefficients $c_{y_{I(2k-1)}}$ and $c_{y_{I(2k)}}$ correspond to the complex conjugate eigenvalue pairs, and c_{y_R} corresponds to the real eigenvalues, respectively. Consider an exponential term to be faster than another when its corresponding eigenvalues are more negative.

$$\begin{aligned} y(t) =& r_0 + \sum_{k=1}^{n_{pair}} c_{y_{I(2k-1)}}(t_i) e^{\alpha_k (t-t_i)} \cos\left(\beta_k (t-t_i)\right) \\ &+ c_{y_{I(2k)}}(t_i) e^{\alpha_k (t-t_i)} \sin\left(\beta_k (t-t_i)\right) \\ &+ \sum_{h=1}^{n_{real}} c_{y_{Rh}}(t_i) e^{\lambda_{Rh}(t-t_i)}, \qquad t \in \langle t_i, t_{i+1}] \end{aligned} \tag{53}$$

Here, the coefficients c_{y_I} and c_{y_R} are defined by:

$$c_{y_{I(2k-1)}}(t_i) = \sum_{l=1}^{n} 2\sigma_{nl,k} \hat{x}_l(t_i) \tag{54}$$

$$c_{y_{I(2k)}}(t_i) = \sum_{l=1}^{n} -2\tau_{nl,k} \hat{x}_l(t_i) \tag{55}$$

$$c_{y_{Rh}}(t_i) = \sum_{l=1}^{n} a_{n(h+n_{imag})} b_{(h+n_{imag})l} \hat{x}_l(t_i) \tag{56}$$

The sine and cosine terms of each complex pair of eigenvalues in (53) can be combined into a single (shifted) sine term:

$$\begin{aligned} y(t) =& r_0 + \sum_{k=1}^{n_{pair}} c_{y_{I(2k-1)(2k)}}(t_i) e^{\alpha_k (t-t_i)} \\ &\sin\left(\beta_k (t-t_i) + \psi_{y(2k-1)(2k)}(t_i)\right) \\ &+ \sum_{h=1}^{n_{real}} c_{y_{Rh}}(t_i) e^{\lambda_{Rh}(t-t_i)}, \qquad t \in \langle t_i, t_{i+1}] \\ =& r_0 + y_{osci}(t) + y_{base}(t), \qquad t \in \langle t_i, t_{i+1}] \end{aligned} \tag{57}$$

In which, $c_{y_{I(2k-1)(2k)}}(t_i) = \sqrt{c_{y_{I(2k-1)}}(t_i)^2 + c_{y_{I(2k)}}(t_i)^2}$ and $\psi_{(2k-1)(2k)}(t_i) = \frac{c_{y_{I(2k-1)}}(t_i)}{c_{y_{I(2k)}}(t_i)}$.

In short, the step response consists of a baseline response $y_{base}(t)$, which is a sum of exponentials belonging to the real eigenvalues decaying to zero over time. The oscillatory term $y_{osci}(t)$ adds an oscillation with decreasing amplitude to the baseline response and is linked to the complex eigenvalue pairs. Over time the total response will tend to $y(t) = r_0$ since both the oscillatory and baseline response will asymptotically go to zero. The more negative the eigenvalue, the faster the exponential term will decay. The longer the time after the last reset, the more dominant the slower exponents will be. Moreover, the coefficients control the magnitude of the oscillatory and exponential terms. The values of the coefficients only change during the reset instances. How the coefficients change during the resets is dependent on $\sigma_{nl,k}$, $\tau_{nl,k}$, $a_{n(h+n_{imag})} b_{(h+n_{imag})l}$, and the state values at reset.

Similarly, the velocity and acceleration response can be written in the same form as (57). The velocity response and its coefficients are defined by:

$$\begin{aligned} \dot{y}(t) =& \sum_{k=1}^{n_{pair}} c_{\dot{y}_{I(2k-1)(2k)}}(t_i) e^{\alpha_k (t-t_i)} \\ &\sin\left(\beta_k (t-t_i) + \psi_{\dot{y}(2k-1)(2k)}(t_i)\right) \\ &+ \sum_{h=1}^{n_{real}} c_{\dot{y}_{Rh}}(t_i) e^{\lambda_{Rh}(t-t_i)}, \qquad t \in \langle t_i, t_{i+1}] \\ =& \dot{y}_{osci}(t) + \dot{y}_{base}(t) \end{aligned} \tag{58}$$

In which,

$$c_{\dot{y}_{I(2k-1)(2k)}}(t_i) = \sqrt{\alpha_j^2 + \beta_j^2}\, c_{y_{I(2k-1)(2k)}}(t_i) \tag{59}$$

$$\psi_{\dot{y}_{I(2k-1)(2k)}}(t_i) = \psi_{y_{I(2k-1)(2k)}}(t_i) + \tan^{-1}\left(\frac{\beta_j}{\alpha_j}\right) \tag{60}$$

$$c_{\dot{y}_{Rh}}(t_i) = \lambda_{Rh} c_{y_{Rh}}(t_i) \tag{61}$$

The acceleration response and its coefficients are described by:

$$\begin{aligned}\ddot{y}(t) = &\sum_{k=1}^{n_{pair}} c_{\ddot{y}_{I(2k-1)(2k)}}(t_i) e^{\alpha_k (t-t_i)} \\ &\sin\left(\beta_k (t-t_i) + \psi_{\ddot{y}(2k-1)(2k)}(t_i)\right) \\ &+ \sum_{h=1}^{n_{real}} c_{\ddot{y}_{Rh}}(t_i) e^{\lambda_{Rh}(t-t_i)}, \qquad t \in \langle t_i, t_{i+1}] \\ &= \ddot{y}_{osci}(t) + \ddot{y}_{base}(t)\end{aligned} \tag{62}$$

In which,

$$c_{\ddot{y}_{I(2k-1)(2k)}}(t_i) = (\alpha_j^2 + \beta_j^2) c_{y_{I(2k-1)(2k)}}(t_i) \tag{63}$$

$$\psi_{\ddot{y}_{I(2k-1)(2k)}}(t_i) = \psi_{y_{I(2k-1)(2k)}}(t_i) + 2\tan^{-1}(\frac{\beta_j}{\alpha_j}) \tag{64}$$

$$c_{\ddot{y}_{Rh}}(t_i) = \lambda_{Rh}^2 c_{y_{Rh}}(t_i) \tag{65}$$

The velocity and acceleration response coefficients depend on the step response coefficients belonging to the same eigenvalue. However, these coefficients are scaled differently depending on the related eigenvalue.

The coefficients defined above characterize the step, velocity, and acceleration response. By looking at the evolution of the coefficients over time, the path of the step response and the plant's energy can be approximated by only taking the dominant exponential terms into account. The dominant exponential terms are the exponents of which the coefficients are significantly larger in magnitude than the coefficients of the other exponents. In the following sections, two approaches are introduced to analyze the damping of reset systems with mass plants. First, the coefficients of the step response itself are used to analyze damping. Subsequently, the power and energy expressions are used to develop an approach to determine the system's damping. Both lead to a similar analysis but achieve it with a slightly different method.

A. Damping analysis: Step response

The damping of the step response can be analyzed directly from the analytic expression of the step response. The damping of a system is higher when overshoot is reduced and the response reaches the reference slower. By increasing the magnitude of decay rate α_k and decreasing the magnitude of $c_{y_{I(2k-1)(2k)}}(t_i)$ in (57), the damping can be increased since the magnitude of the oscillatory components is reduced. Moreover, the coefficients $c_{y_{Rh}}(t_i)$ in (57) determine the time it takes the baseline response to vanish. When the slower exponential terms (smallest $|\lambda_{Rh}|$) are dominant and have negative coefficients, the baseline response will decay slowly and from below zero. The slower the dominant exponential terms are, the more damped the step response will be because the system has more time to reduce the oscillations before overshoot occurs. Note that the amount that the coefficients can change between resets is bounded by the change of the plant's location since the plant location in (53) at reset is defined by (66). Therefore, a dominant exponential term will always be accompanied by another dominant exponential term whose coefficient is of the opposite sign.

$$y(t_i) = r_0 + \sum_{k=1}^{n_{pair}} c_{y_{I(2k-1)}}(t_i) + \sum_{h=1}^{n_{real}} c_{y_{Rh}}(t_i) \tag{66}$$

The step response's damping can be assessed by looking at the coefficients' evolution. One can use the following steps as a guideline for analyzing the damping of the reset control system.

1) Calculate the eigenvalues and eigenvectors of the system matrix A_{cl}.
2) Calculate the values of coefficients $c_{y_{I(2k-1)(2k)}}(t_i)$ and $c_{y_{Rh}}(t_i)$ for reset instances t_i. Here $h = 1, 2, ..., n_{real}$
3) Identify the dominant exponential terms based on the magnitude of the coefficients.
4) For the significant oscillatory coefficients: the quicker the coefficient is reduced to zero, the quicker the oscillations are removed from the response. The slower oscillatory terms should be reduced faster to achieve a damped response since their effect is the most persistent.
5) For the baseline coefficients: consider only the dominant baseline terms. If the coefficient of the slowest dominant exponential term is negative, the response will be better damped and will not likely overshoot. By contrast, if the coefficient of the slowest exponential term is positive, the response will be damped less. Moreover, the slower the most dominant term, the more the system is damped.

Note that the coefficients are only changed during reset instances. With a shaping filter, the reset instances could be designed so that the coefficients are updated beneficially. Moreover, the evolution of the coefficients is dependent on the eigenvectors of the system matrix. These determine the weights of the states in the calculation of the coefficients (54)-(56). By changing controller parameter values or configuration, the eigenvectors could be designed to favor a particular state in calculating the step response coefficient. Lastly, the states can be designed to favorably influence the coefficients by changing parameter values and controller configuration.

B. Damping analysis: Energy and Power

As mentioned in Section III-A, the controller dampens the system when it applies negative power to the plant. In general, the controller should apply sufficient negative power to the system to dissipate all energy exactly when it reaches the reference to prevent overshoot.

For the controller to apply negative power, the acceleration and velocity terms in (25) should have the opposite sign. Therefore, negative acceleration is required to remove the initial kinetic energy needed to move the plant toward the reference in the step response.

In (62)-(65), the acceleration response and its coefficients are defined. The coefficient of the oscillatory terms should be reduced when damping is required. Otherwise, the power will eventually become positive and add energy to the system. Due to the exponential decay of the baseline response, the coefficients of the slowest dominant exponential terms should be negative to prevent the power from becoming positive. The dominant exponential terms are those whose coefficients have significant magnitude compared to the other coefficients. In contrast to the step response, the acceleration response is not necessarily continuous. Therefore, the acceleration (and power) can change instantaneously during reset. Consequently, the coefficients change with it according to (67). Therefore, the coefficient sum should be the opposite sign of the velocity for the controller to apply damping after reset.

$$\begin{aligned}\ddot{y}(t_i) = &\sum_{k=1}^{n_{pair}} c_{\ddot{y}_{I(2k-1)(2k)}}(t_i)\sin\left(\psi_{\ddot{y}_{I(2k-1)(2k)}}(t_i)\right) \\ &+ \sum_{h=1}^{n_{real}} c_{\ddot{y}_{Rh}}(t_i)\end{aligned} \tag{67}$$

Note that $c_{\ddot{y}_{I(2k-1)(2k)}}$ and $c_{\ddot{y}_{Rh}}$ are scaled versions of $c_{y_{I(2k-1)(2k)}}$ and $c_{y_{Rh}}$. The coefficients are scaled by the square of corresponding eigenvalues (63), (65). The acceleration coefficients of fast exponential terms will become more dominant than the step coefficients since they are scaled more.

By looking at the coefficients $c_{\ddot{y}}$, one can analyze the damping of the reset controller. The following steps can be used as a guideline for analyzing the damping of the step response in a reset control system:

1) Calculate the eigenvalues and eigenvectors of the system matrix A_{cl}.
2) Calculate the values of coefficients $c_{\ddot{y}_{I(2k-1)(2k)}}(t_i)$ and $c_{\ddot{y}_{Rh}}(t_i)$ for reset instances t_i.
3) Identify the dominant exponential terms based on the magnitude of the coefficients.
4) For the significant oscillatory coefficients: the quicker the coefficients are reduced, the quicker the oscillations are removed from the response. The presence of oscillations in power will lead to the addition of energy at some point, which causes a loss of damping.
5) For the baseline coefficients: consider only the dominant baseline terms. If the sum of coefficients in (67) is negative, the controller will dissipate energy directly after the reset. Then the damping will be applied longer if the coefficient of the slowest dominant exponential term is negative. Therefore, the response will be more damped and less likely to overshoot. By contrast, if the coefficient of the slowest exponential term is positive, energy will be increased again, which decreases the damping. Finally, the slower the most dominant exponential term, the longer the controller provides damping if the coefficient is negative.

Note that the coefficients $c_{\ddot{y}}$ could be designed similarly to coefficients c_y since they are proportional to each other. However, the exact value of the eigenvalues is relevant for tuning $c_{\ddot{y}}$ since coefficients of the faster exponential terms will be scaled more.

In short, one can use the step response and power expressions to analyze the damping in a reset control system with stable BLS controlling a mass plant.

V. Illustrative example: Damping analysis of CgLp-PID

To illustrate the use of the damping analyses introduced in Section IV, consider the CgLp-PID controlling a mass plant in Fig. 3. [11] and [24] have shown the dependency of the step response on the sequence of control elements. Moreover, both [11], and [24] show that in a CgLp element, it could be beneficial to use a Lead-Reset configuration compared to a Reset-Lead configuration. The Lead-Reset sequence can provide more damping to the system and reduce overshoot for the same phase margin. The CgLp-PID damping analysis provides insight into the additional damping attained by the Lead-Reset configuration.

The Lead element of a conventional CgLp (see Section II) is split into two separate lead elements in Fig. 3. By changing the value of ω_l, the lead strength can be changed before and after the reset block. The lead after the reset element will vanish when ω_l is close to ω_r, which results in a Lead-Reset configuration. Similarly, the lead before the reset element will disappear when ω_l approaches ω_f, which results in a Reset-Lead configuration. Therefore, ω_l can control the lead placement in the CgLp element. In this example, the damping of the step response is analyzed for different ω_l values. Since the first-order DF is independent of ω_l, all the changes in damping can be attributed to the lead placement because the phase margin will be equal for all controllers.

The controller is tuned such that the BLS is stable and has a small phase margin of 5° at a bandwidth frequency of $f_c = 100Hz$. Full reset ($\gamma = 0$) is chosen for simplicity. The correction factor α_s is taken to be 1.62 according to [10]. The CgLp element is tuned to provide phase lead over an extensive frequency range, such that the effect of the location of the lead element is significant when sweeping ω_l over this range. Through the broadband phase lead provided by the CgLp, the phase margin of the RCS is 55°. Therefore, the RCS is expected to provide more damping than the BLS. The controller and system parameters are listed in Table I.

Consider the states of the system to be defined as follows:

$$\hat{x}(t) = \begin{bmatrix}\hat{x}_r & \hat{x}_{L1} & \hat{x}_{L2} & \hat{x}_D & \hat{x}_{PIplant}\end{bmatrix}^T \tag{68}$$

Here, $\hat{x}_r$ is the state of the reset element. $\hat{x}_{L1}$, $\hat{x}_{L2}$, and $\hat{x}_D$ are the states of the lead elements before the reset element, after the reset element, and in the PID. The combined PI controller and mass plant states are $\hat{x}_{PIplant}$. Then the system can be described by (69)-(72).

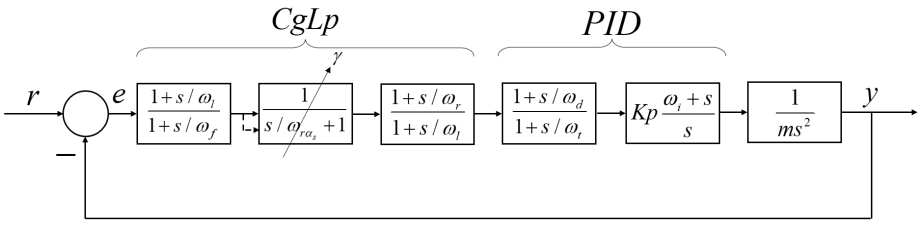

Fig. 3: Diagram of CgLp-PID controlling a mass plant.

TABLE I: Control and system parameters of CgLp-PID with a mass plant.

Symbol	Description	Value
ω_c	Bandwidth frequency	100 Hz
ω_r	Corner frequency of lead filter in CgLp	$\omega_c/6$
ω_f	Taming frequency of lead filter in CgLp	$10\omega_c$
α_s	Correction factor reset element	1.62
$\omega_{r\alpha_s}$	Corner frequency of reset element	ω_r/α_s
ω_i	Corner frequency of lag filter in PID	$\omega_c/10$
ω_d	Corner frequency of lead filter in PID	$\omega_c/1.5$
ω_t	Taming frequency of lead filter in PID	$1.5\omega_c$
K_p	Proportional gain in PID	1432
m	Mass of mass plant	5e-3 kg
r_0	Step amplitude	1 μm
ω_l	Lead location parameter	$[\omega_r, \omega_f]$

$$A_{cl} = \begin{bmatrix} -\omega_{r\alpha_s} & \omega_{r\alpha_s} & 0 & 0 & 0 & 0 & -\omega_{r\alpha_s}\frac{\omega_f}{\omega_l} \\ 0 & -\omega_f & 0 & 0 & 0 & 0 & -\omega_f(1-\frac{\omega_f}{\omega_l}) \\ \omega_l(1-\frac{\omega_l}{\omega_r}) & 0 & -\omega_l & 0 & 0 & 0 & 0 \\ \frac{\omega_l\omega_t}{\omega_r}(1-\frac{\omega_t}{\omega_d}) & 0 & \omega_t(1-\frac{\omega_t}{\omega_d}) & -\omega_t & 0 & 0 & 0 \\ \frac{\omega_l\omega_t}{\omega_r\omega_d}\frac{K_p\omega_i}{m} & 0 & \frac{\omega_t}{\omega_d}\frac{K_p\omega_i}{m} & \frac{K_p\omega_i}{m} & 0 & 0 & 0 \\ \frac{\omega_l\omega_t}{\omega_r\omega_d}\frac{K_p}{m} & 0 & \frac{\omega_t}{\omega_d}\frac{K_p}{m} & \frac{K_p}{m} & 1 & 0 & 0 \\ 0 & 0 & 0 & 0 & 0 & 1 & 0 \end{bmatrix} \tag{69}$$

$$C_{cl} = \begin{bmatrix} 0 & 0 & 0 & 0 & 0 & 0 & 1 \end{bmatrix} \tag{70}$$

$$C_{rline} = \begin{bmatrix} 0 & 1 & 0 & 0 & 0 & 0 & -\frac{\omega_f}{\omega_l} \end{bmatrix} \tag{71}$$

$$\hat{A}_\rho = \begin{bmatrix} \gamma & 0 \\ 0 & I^{6\times 6} \end{bmatrix} \tag{72}$$

The eigenvalues of the system matrix of the CgLp-PID are given by (73). Note that the first six eigenvalues are independent of the location of the lead filter in the CgLp. As intended, all eigenvalues have a negative real part, making the BLS stable.

$$\lambda = \begin{bmatrix} -29.8 + 492.4 \\ -29.8 - 492.4 \\ -6350.1 \\ -719.1 \\ -98.8 \\ -62.8 \\ -\omega_l \end{bmatrix} \tag{73}$$

With the use of (41), the step response can be determined analytically for different lead location parameter values ω_l.

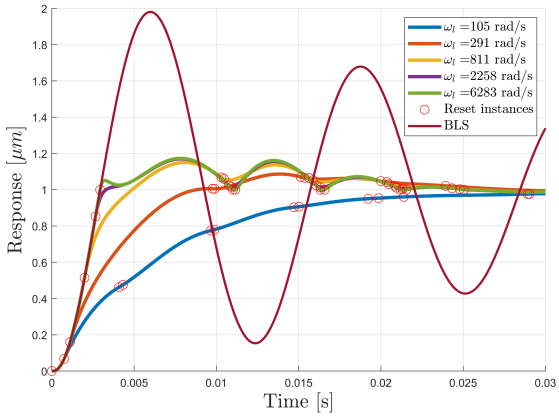

Fig. 4: Step response of CgLp-PID with mass plant for different ω_l values.

Assume that the systems are entirely at rest when $t = 0$. The initial state of the system will then be $\hat{x}(0) = \begin{bmatrix} 0^{6\times 1} \\ -r_0 \end{bmatrix}$. The step responses of the different controllers are shown in Fig. 4. The percentage overshoot of the CgLp-PID compared to the BLS as a function of ω_l can be seen in Fig. 5. The reset implementation decreases the system's overshoot through the extra phase margin. Additionally, the overshoot is decreased further when more lead is placed before the reset element, like in [11] and [24]. In a small frequency range ($\omega_l \in [\omega_r, 135]$), the overshoot is prevented entirely. The following sections analyze how the system provides more damping for lower ω_l values.

A. Damping analysis: step response

In this section, the step response damping analysis from Section IV is used to see how the lead placement changes the damping of the step response. The step response of the CgLp-PID consists of one oscillatory term and five baseline exponential terms (74)-(76).

$$y(t) = r_0 + y_{osci}(t) + y_{base}(t), \qquad t \in \langle t_i, t_{i+1}] \tag{74}$$

In which,

$$\begin{aligned} y_{osci}(t) = {} & c_{y_{I12}}(t_i)e^{-29.8(t-t_i)} \\ & \sin(492.4(t-t_i) + \psi_{y_{I12}}(t_i)), \qquad t \in \langle t_i, t_{i+1}] \end{aligned} \tag{75}$$

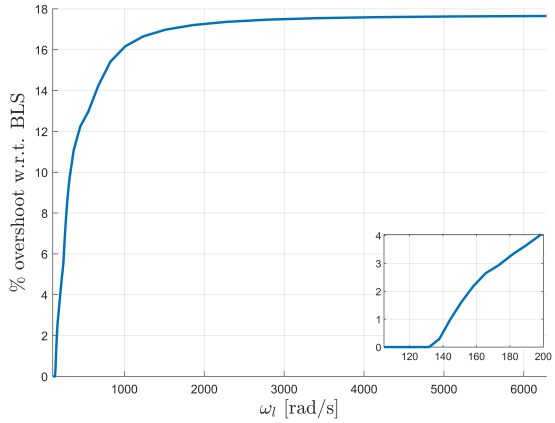

Fig. 5: Percentage overshoot in step response of CgLp-PID compared to BLS for different ω_l values.

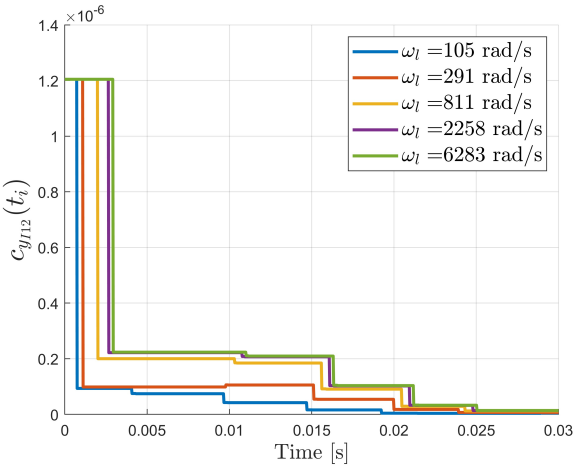

Fig. 6: Oscillatory coefficient evolution for different ω_l.

$$\begin{aligned} y_{base}(t) = {} & c_{y_{R1}}(t_i)e^{-6350.1(t-t_i)} \\ & + c_{y_{R2}}(t_i)e^{-719.1(t-t_i)} + c_{y_{R3}}(t_i)e^{-98.8(t-t_i)} \\ & + c_{y_{R4}}(t_i)e^{-62.8(t-t_i)} + c_{y_{R5}}(t_i)e^{-\omega_l(t-t_i)}, \\ & t \in \langle t_i, t_{i+1}] \end{aligned} \tag{76}$$

Firstly, the coefficient $c_{y_{I12}}$ and the decay rate α determine the amplitude of the oscillatory content. Note that the magnitude of α is low compared to the other eigenvalues. Therefore, the reduction of $c_{y_{I12}}$ will be vital for reducing the amplitude of the oscillations before it leads to overshoot. In Fig. 6 can be seen that the coefficient is reduced more and earlier in the response when more lead is before the reset element. The earlier reduction can partially be attributed to the earlier reset of these systems. However, the oscillatory term is also reduced more in controllers with lower ω_l when the first reset happens simultaneously. In Fig. 7, all systems have the same t_1. Here, the reduction of the oscillation coefficient is still greater for lower ω_l. In short, the more lead is placed before the reset element, the more and faster the oscillatory content of the step response is damped.

Secondly, the coefficients c_{y_R} determine which exponential terms are relevant for the baseline response. From Fig. 8, it can be concluded that $c_{y_{R2}}$, $c_{y_{R3}}$, and $c_{y_{R5}}$ are the dominant exponential terms to approximate the baseline response. The exponential term with coefficient $c_{y_{R1}}$ becomes significant when $\omega_l = 6283 rad/s$. However, its effect on the step response will be little since the corresponding eigenvalue λ_{R1} is large compared to the other dominant exponents. Therefore, the exponential term with coefficient $c_{y_{R1}}$ will be neglected in this analysis. Generally, the more lead is placed after the reset element, the more dominant the faster exponents will be. Faster dominant exponential terms cause the baseline response to become faster, which limits the time the oscillatory coefficient has to be decreased. Therefore, overshoot is more likely and severe when more lead is after the reset

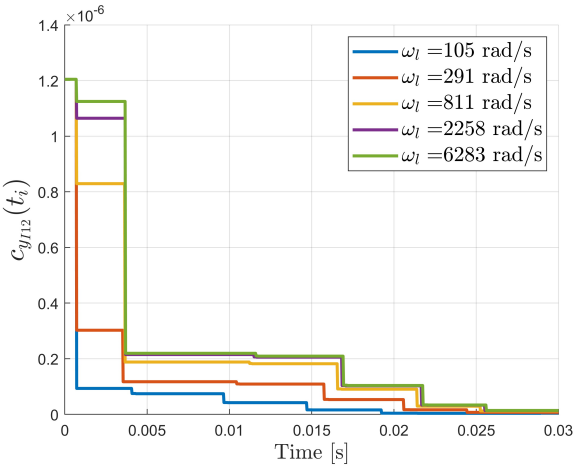

Fig. 7: Oscillatory coefficient evolution for different ω_l when t_1 is fixed.

element. Note that ω_l determines the decay rate of the exponential corresponding to λ_{R5}. Therefore, the baseline response of the coefficients in Fig. 8d will be faster than in Fig. 8c.

The step response of each system can be approximated by $\tilde{y}(t) = y_{osci}(t) + \tilde{y}_{base}(t)$. Here, $\tilde{y}_{base}(t)$ is composed of the dominant exponents in (77). The composition of the approximated step response can be seen in Fig. 9. In short, from the analysis of the step response coefficients can be concluded that the step response is less damped the more lead is after the reset element. The oscillation coefficient has been reduced less when the baseline response approaches zero, and a faster baseline response is caused by the faster exponential terms being more dominant when ω_l increases. The maximal and root mean square (RMS) error values $\tilde{e}(t)$ are given in Table II to show the accuracy of the approximation. Here, the approximation error is given by $\tilde{e}(t) = y(t) - \tilde{y}(t)$.

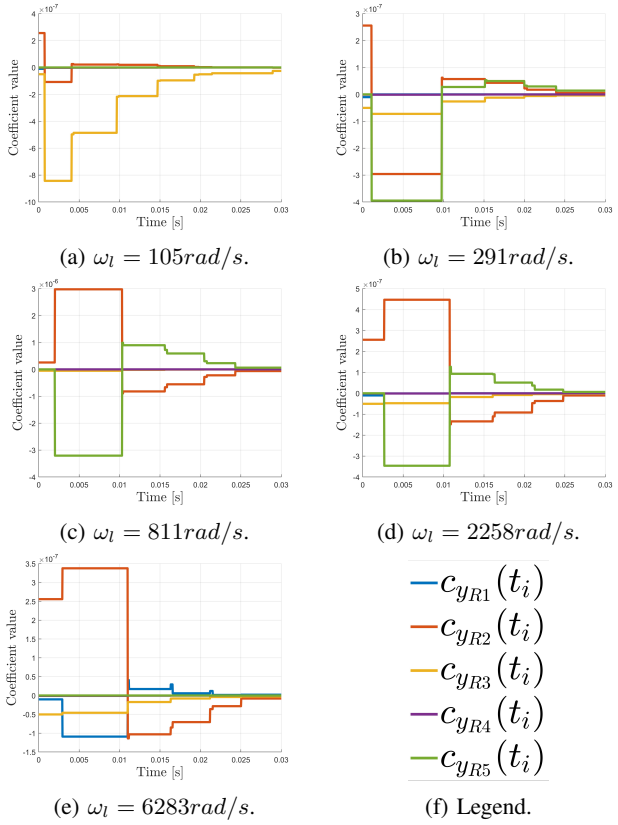

(a) $\omega_l = 105 rad/s$. (b) $\omega_l = 291 rad/s$. (c) $\omega_l = 811 rad/s$. (d) $\omega_l = 2258 rad/s$. (e) $\omega_l = 6283 rad/s$. (f) Legend.

Fig. 8: Baseline coefficients for different ω_l values.

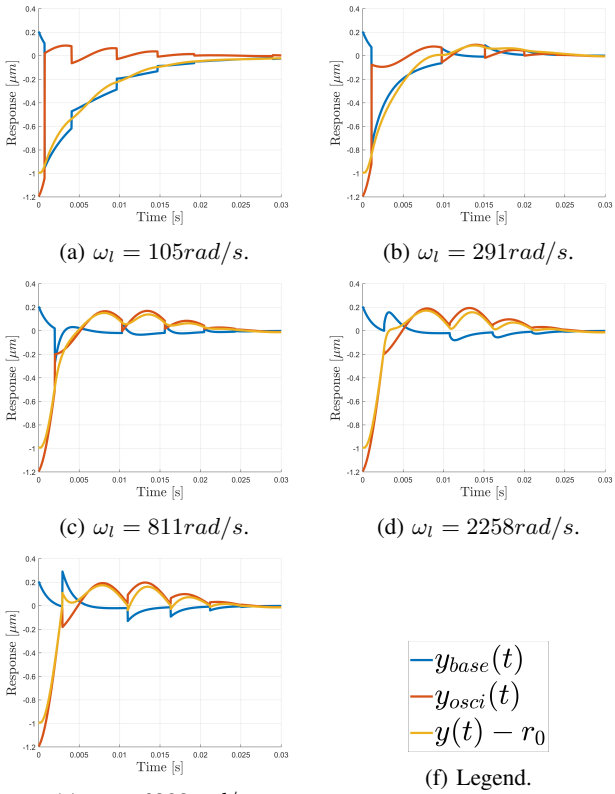

(a) $\omega_l = 105 rad/s$. (b) $\omega_l = 291 rad/s$. (c) $\omega_l = 811 rad/s$. (d) $\omega_l = 2258 rad/s$. (e) $\omega_l = 6283 rad/s$. (f) Legend.

Fig. 9: Approximation of the step response $y(t)$ as the sum of the oscillatory term $y_{osci}(t)$ and the dominant baseline terms $y_{base}(t)$.

$$\tilde{y}_{base}(t) = c_{y_{R2}}(t_i)e^{-719.1(t-t_i)} + c_{y_{R3}}(t_i)e^{-98.8(t-t_i)} + c_{y_{R5}}(t_i)e^{-\omega_l(t-t_i)}, \quad t \in \langle t_i, t_{i+1}] \tag{77}$$

It can be concluded that the dominant exponential terms can approximate the step response of this system well since the RMS error value does not exceed 1% of the step height. Note that the maximum error for the system where $\omega_l = \omega_f$ is more significant than in the other systems because the baseline exponential term with coefficient $c_{y_{R1}}$ is not considered in the approximation. Since this baseline term decays fast, it only leads to significant errors during the resets, as seen in Fig. 10. However, the approximation can still be used to analyze the system's damping since the RMS error is less than 1%.

B. Damping analysis: energy and power

In this section, the energy and power damping analysis method introduced in Section IV is used to analyze how the lead placement changes the damping of the step response. For the system to be adequately damped, all plant energy should be dissipated when the reference is reached, as mentioned in Section IV-B. The plant will overshoot when insufficient energy is dissipated, which is defined mathematically in (78). Here, $t_{E=0}$ is when all plant energy at the first reset $E(t_1)$ is dissipated. $t_{y=r_0}$ is the instance when the

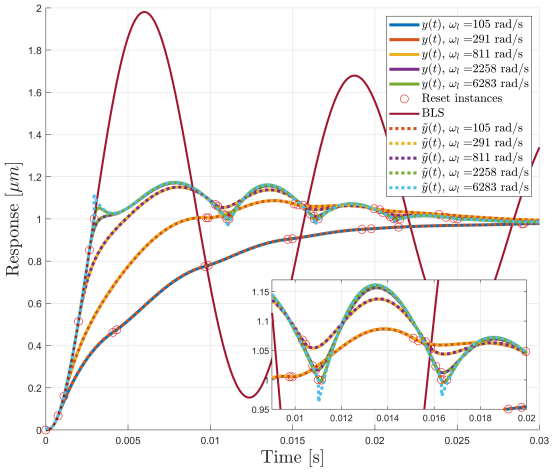

Fig. 10: Approximation of the step response and the step response of CgLp-PID with mass plant system for different ω_l.

TABLE II: Error of approximation of step response by using the oscillatory terms, and baseline terms corresponding to λ_{R2}, λ_{R3}, and λ_{R5}.

Lead placement	$\omega_l = 105 rad/s$	$\omega_l = 291 rad/s$	$\omega_l = 811 rad/s$	$\omega_l = 2258 rad/s$	$\omega_l = 6283 rad/s$
$\tilde{e}_{RMS}$ [μm]	0.0014	0.0010	0.0009	0.0009	0.0066
max($\lvert\tilde{e}(t)\rvert$) [μm]	0.0114	0.0114	0.0114	0.0114	0.1060

output crosses the reference for the first time. To prevent overshoot $t_{E=0}$ should be equal to $t_{y=r_0}$.

$$E(t_1) - \int_{t_1}^{t_{E=0}} P(t)dt = 0 \tag{78}$$

The reset instances are determined by the output of the first lead filter since no shaping filter is applied. Earlier resets could be advantageous to limit the plant energy at the first reset instance. When $\omega_l = \omega_f$ the resets will occur when $y(t_i) = r_0$. The late reset will inherently result in overshoot since the system contains a slowly decaying oscillatory term. Therefore, implementing a shaping filter could be beneficial to reset the controller earlier when ω_l is close to ω_f. When more lead is in front of the reset element, earlier resets are expected since the reset instances by approximation depend on the linear combination of the output and velocity response when $\omega_f \gg \omega_l$ [11]. Therefore, lower ω_l could be advantageous to limit the amount of plant energy in the first reset instance when no shaping filter is present.

In line with Section IV-B, the acceleration coefficients $c_{\ddot{y}}$ are determined to analyze the energy dissipation of the controllers. The acceleration response of the CgLp-PID consists of one oscillatory term and five exponential baseline terms (79)-(81).

$$\ddot{y}(t) = r_0 + \ddot{y}_{osci}(t) + \ddot{y}_{base}(t), \qquad t \in \langle t_i, t_{i+1}] \tag{79}$$

In which,

$$\begin{aligned}\ddot{y}_{osci}(t) = {} & c_{\ddot{y}_{I12}}(t_i)e^{-29.8(t-t_i)} \\ & \sin(492.4(t-t_i) + \psi_{\ddot{y}_{I12}}(t_i)), \qquad t \in \langle t_i, t_{i+1}]\end{aligned} \tag{80}$$

$$\begin{aligned}\ddot{y}_{base}(t) = {} & c_{\ddot{y}_{R1}}(t_i)e^{-6350.1(t-t_i)} \\ & + c_{\ddot{y}_{R2}}(t_i)e^{-719.1(t-t_i)} + c_{\ddot{y}_{R3}}(t_i)e^{-98.8(t-t_i)} \\ & + c_{\ddot{y}_{R4}}(t_i)e^{-62.8(t-t_i)} + c_{\ddot{y}_{R5}}(t_i)e^{-\omega_l(t-t_i)}, \\ & t \in \langle t_i, t_{i+1}]\end{aligned} \tag{81}$$

Firstly, the sum of the coefficients in (67) determines the acceleration after reset. The sum for the different controllers is provided in Fig. 11. The more lead is after the reset element, the more acceleration changes during reset. In the first reset, all the controllers provide negative acceleration. Therefore, the controller instantaneously provides more damping during the first reset when ω_l is greater.

Moreover, the coefficient $c_{\ddot{y}_{I12}}$ determines the amplitude of the oscillations of the controller power. The evolution of $c_{\ddot{y}_{I12}}$ for different ω_l can be seen in Fig. 12. The more lead is before the reset element, the more the oscillations are reduced. Note that the faster oscillation reduction can

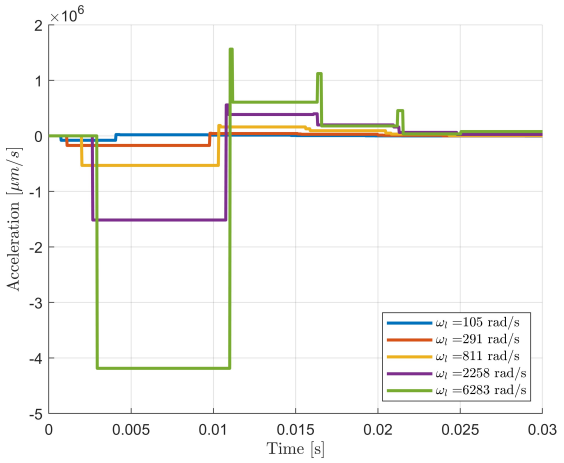

Fig. 11: Acceleration after last reset for different ω_l.

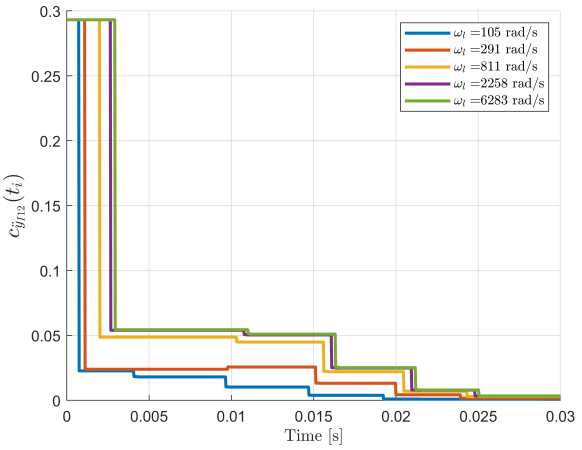

Fig. 12: Oscillatory coefficient value for different ω_l.

be partially attributed to the earlier reset for lower ω_l. However, the oscillations are also reduced less when the first reset is equal for all systems, as shown in Fig. 7 in the previous section. In general, when more lead is after the reset element, oscillations in the power expression could cause the energy to increase again and cause overshoot.

Finally, the coefficients $c_{\ddot{y}_R}(t_i)$ determine the baseline acceleration response. The coefficients for the different lead placements can be seen in Fig. 13. The significant coefficients for the acceleration response are $c_{\ddot{y}_{R1}}$, $c_{\ddot{y}_{R2}}$, and $c_{\ddot{y}_{R5}}$. Note that $c_{\ddot{y}_{R5}}$ is only significant when ω_l is large and represents a fast exponential term. The more lead is present before the reset element, the more dominant the

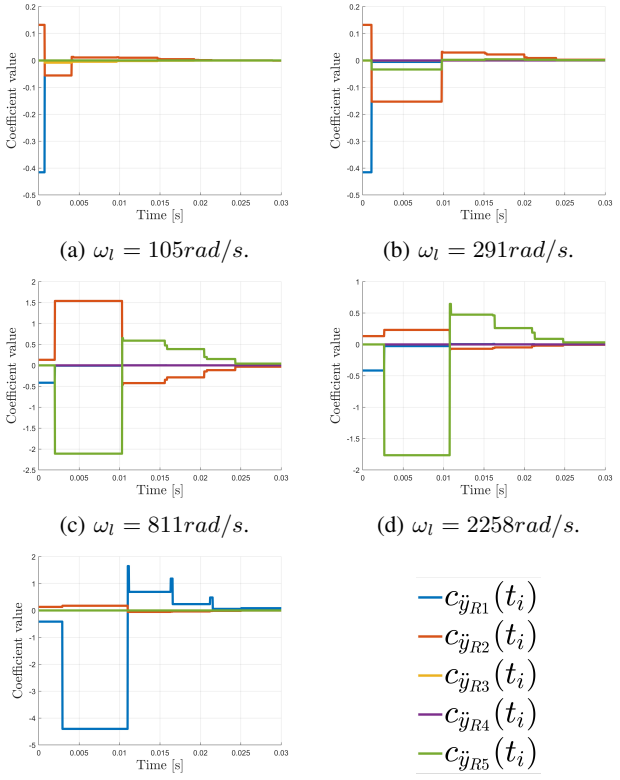

(a) $\omega_l = 105rad/s$. (b) $\omega_l = 291rad/s$.

(c) $\omega_l = 811rad/s$. (d) $\omega_l = 2258rad/s$.

(e) $\omega_l = 6283rad/s$. (f) Legend.

Fig. 13: Approximation of the step response $y(t)$ as the sum of the oscillatory term $y_{osci}(t)$ and the dominant baseline terms $y_{base}(t)$.

faster exponential terms will become, which suggests a fast decay of power. Therefore, the higher ω_l, the faster the damping will vanish.

In short, the damping of the CgLp-PID controller is expected to be instantaneously higher in the first reset for higher ω_l. However, the higher ω_l, the faster the baseline acceleration and power decay. Therefore, lead after reset provides high but short damping. In contrast, lead before reset provides low but sustained damping. Moreover, more significant acceleration oscillations can cause overshoot due to the power becoming positive. Combined with the earlier reset, the step response will be damped more when ω_l.

The plant energy and power for different ω_l can be seen in Fig. 14 and 15, which validates the conclusion of the coefficient analysis. Especially the late first reset and the oscillations in power cause the overshoot of the step response. Enough energy is dissipated only when ω_l is sufficiently low (78).

Both step response and energy analysis show that the oscillatory content is reduced the more lead is located before the reset element. The decrease in oscillations can be attributed to the reduction of the higher-order harmonics in the open-loop frequency response of the system shown

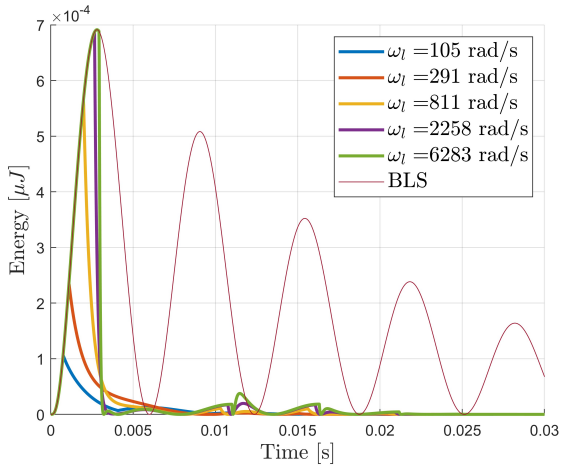

Fig. 14: Plant energy of CgLp-PID with mass plant for different ω_l.

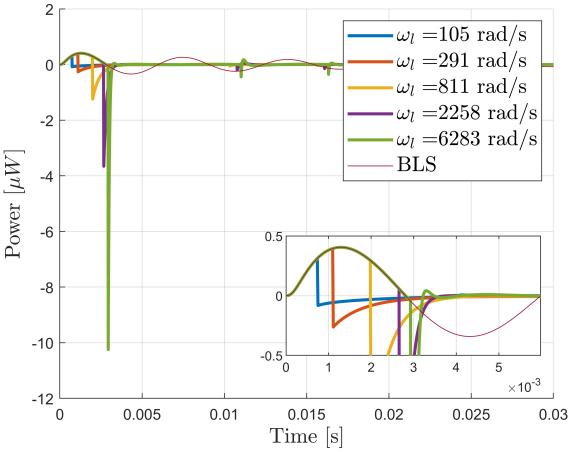

Fig. 15: Controller power of CgLp-PID with mass plant for different ω_l.

in Fig. 16. The third and fifth harmonics are reduced in magnitude at oscillation frequency $\beta = 492rad/s$ for lower values of ω_l, reducing the amplitude of the oscillations more at that frequency. In general, the higher-order harmonics should be reduced at oscillation frequencies in the response (given by the imaginary part β of the complex eigenvalues) for the response to be damped more.

In short, the step response and energy analysis show that the system is more damped when more lead is located before the reset element, similar to what was found in [11], [24]. Therefore, using a Lead-Reset configuration in a CgLp-PID controller with a mass plant is beneficial to reduce and prevent overshoot. At the same time, the settling time remains approximately constant, as seen in Fig. 4. Note that the rise time will be increased when more lead is placed before the reset. When a maximum rise time is required, placing more lead after the reset element could be beneficial.

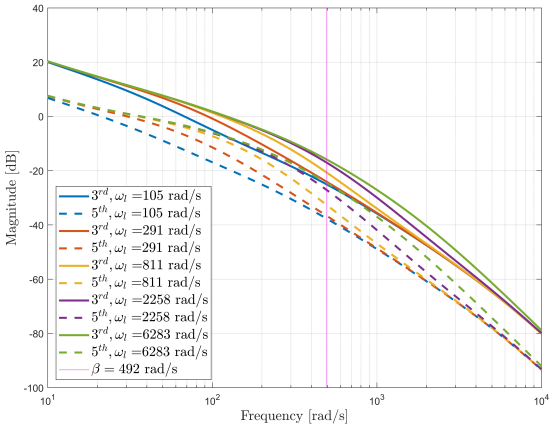

Fig. 16: HOSIDFs of open-loop CgLp-PID with mass plant system for different ω_l.

VI. Conclusions and Future Work

A reset control system's response depends on the exact controller configuration. The dependence on the controller sequence changes the damping of the response without influencing the first-order frequency response. Therefore, the amount of damping in a reset control system cannot be captured only regarding the phase margin. Currently, the step response is calculated numerically to see the effect of different controller element sequences on the transient response. However, this does not provide insight into the underlying cause of the additional damping. This paper proposes an analytical approach to analyze the damping of the transient response of reset control systems controlling a mass plant. The approach provides a method to explore how different controller configurations with the same control elements change the damping of the step response.

First, the step response and its derivatives are derived for reset control systems with mass plants. The analytical expressions are used to analyze the damping of the step response in reset control systems with stable base linear systems. By reducing oscillatory terms and making slower exponential terms more dominant, the damping of the step response can be increased. Additionally, analyzing the controller's energy dissipation can provide insight into the damping of the step response. By delivering sustained negative power, energy can be dissipated such that overshoot is prevented. Similar to the step response, oscillations should be reduced for the response to be damped.

To show the value of the proposed methods, the damping in a CgLp-PID controlling a mass plant is analyzed. It was shown that the damping of the step response could be increased by placing the CgLp lead element before the reset element, reducing oscillations faster and making slower exponential terms more dominant. The oscillation is reduced more since the magnitude of the higher-order harmonics is lower at the oscillation frequency.

To use the proposed damping analysis methods, the base linear system should contain at least one integrator. When mass-spring-damper plants are considered, the analytical derivation should be altered, or an additional integrator should be added. Moreover, the proposed energy analysis assumes the plant to be a single mass. More work is needed to extend this method to account for more complex plants.

Furthermore, this paper only provides insight into the underlying mechanics of damping in reset control systems. The CgLp-PID example shows that the reduction of higher-order harmonics at the response oscillation frequency increases damping. More work is to be done on how to design higher-order harmonics to enhance transient performance. The tuning of the reset instances, eigenvalues, and eigenvectors of the system should be considered when developing novel tuning guidelines.

Furthermore, more work is needed to be done to gain insight into the dependence of damping on high-order harmonics. The added damping through the reduction of higher-order harmonics holds for the CgLp-PID example. A more rigid theory is to be formulated, which would offer the possibility to formulate new tuning guidelines for transient performance in reset control.

Finally, the analytical expressions could provide a way to develop a novel way of defining the stability of a reset control system. Stability could be guaranteed if a specific system decreases the overall system's energy during reset instances. This could especially be interesting if stable reset systems with unstable BLS could be included since these are excluded when the H_β condition is used to asses stability properties [20].

Appendix

A. Matrix entries system matrix RCS system

The entries of the system matrices A_{cl} and B_{cl} can be derived for the general RCS in Fig. 2 from (12)-(21).

$$A_{cl} = \begin{bmatrix} A_{cl11} & A_{cl12} & A_{cl13} & A_{cl14} \\ A_{cl21} & A_{cl22} & A_{cl23} & A_{cl24} \\ A_{cl31} & A_{cl32} & A_{cl33} & A_{cl34} \\ A_{cl41} & A_{cl42} & A_{cl43} & A_{cl44} \end{bmatrix}, \quad B_{cl} = \begin{bmatrix} B_{cl1} \\ B_{cl2} \\ B_{cl3} \\ B_{cl4} \end{bmatrix} \tag{82}$$

Where,

$$A_{cl11} = A_r \tag{83}$$

$$A_{cl12} = B_r C_{c_1} \tag{84}$$

$$A_{cl13} = 0^{n_r \times n_{sf}} \tag{85}$$

$$A_{cl14} = -D_{c_1} B_r C_{c_2 p} \tag{86}$$

$$A_{cl21} = 0^{n_1 \times n_r} \tag{87}$$

$$A_{cl22} = A_{c_1} \tag{88}$$

$$A_{cl23} = 0^{n_1 \times n_{sf}} \tag{89}$$

$$A_{cl24} = -B_{c_1} C_{c_2p} \tag{90}$$

$$A_{cl31} = 0^{n_{sf} \times n_r} \tag{91}$$

$$A_{cl32} = B_{sf} C_{c_1} \tag{92}$$

$$A_{cl33} = A_{sf} \tag{93}$$

$$A_{cl34} = -D_{c_1} B_{sf} C_{c_2p} \tag{94}$$

$$A_{cl41} = B_{c_2p} C_r \tag{95}$$

$$A_{cl42} = D_r B_{c_2p} C_{c_1} \tag{96}$$

$$A_{cl43} = 0^{n_2 \times n_{sf}} \tag{97}$$

$$A_{cl44} = A_{c_2p} - D_{c_1} D_r B_{c_2p} C_{c_2p} \tag{98}$$

$$B_{cl1} = D_{c_1} B_r \tag{99}$$

$$B_{cl2} = B_{c_1} \tag{100}$$

$$B_{cl3} = D_{c_1} B_{sf} \tag{101}$$

$$B_{cl4} = D_{c_1} D_r B_{c_2p} \tag{102}$$

B. Proof transform equality

In this appendix the proof of Lemma 2 is showed with intermediate steps

The Lemma states that systems (22) and (27) are equivalent under state transformation $\hat{x}(t) = x(t) - x_0$ when considering a constant reference for a system where $C_2P(s)$ contains at least 1 integrator.

Here, $x_0 = \begin{bmatrix} 0^{n-n_2} & x_{c_2p0} \end{bmatrix}^T$. Substituting the state transformation in the transformed system gives:

$$\begin{cases} \dot{x} - \dot{x}_0 = A_{cl} x(t) - A_{cl} x_0, & \text{if } u_{sf}(t) \neq 0 \quad (103) \\ x(t^+) - x_0 = \hat{A}_\rho x(t) - \hat{A}_\rho x_0, & \text{if } u_{sf}(t) = 0 \quad (104) \\ y(t) = C_{cl} x(t) - C_{cl} x_0 + r_0 & (105) \\ u_{sf}(t) = C_{rline} x(t) - C_{rline} x_0 & (106) \end{cases}$$

We rewrite each equation separately to find the system in (22).

a) Equation (103): For the first equation, use the fact that $\dot{x}_0 = 0$ and that the expressions of the entries of A_{cl} are provided in Appendix A. Furthermore, use the equations in Lemma 1. Then we can rewrite the first equation of system (22) to:

$$\begin{aligned} \dot{x} &= A_{cl} x - A_{cl} x_0 \\ &= A_{cl} x + \begin{bmatrix} D_{c_1} B_r C_{c_2p} \\ B_{c_1} C_{c_2p} \\ D_{c_1} B_{sf} C_{c_2p} \\ -A_{c_2p} + D_{c_1} D_r B_{c_2p} C_{c_2p} \end{bmatrix} x_{c_2p0} \\ &= A_{cl} x + \begin{bmatrix} D_{c_1} B_r \\ B_{c_1} \\ D_{c_1} B_{sf} \\ D_{c_1} D_r B_{c_2p} \end{bmatrix} r_0 \end{aligned} \tag{107}$$

From Appendix A, the expression of B_{cl} can be retrieved:

$$B_{cl} = \begin{bmatrix} D_{c_1} B_r \\ B_{c_1} \\ D_{c_1} B_{sf} \\ D_{c_1} D_r B_{c_2p} \end{bmatrix} \tag{108}$$

Therefore the first equation of systems (22) and (27) are equivalent.

b) Equation (104): For equation (104) it is straightforward, that $\hat{A}_\rho x_0 = 0$. Therefore, the second equation of systems (22) and (27) are equivalent.

c) Equation (104): For the third equation, use the expression of C_{cl} in (23) and the equations in Lemma 1, to find that:

$$\begin{aligned} y(t) &= C_{cl} x(t) - C_{cl} x_0 + r_0 \\ &= C_{cl} x(t) - C_{c_2p} x_{c_2p0} + r_0 \\ &= C_{cl} x(t) \end{aligned} \tag{109}$$

Therefore, the third equation of systems (22) and (27) are equivalent.

d) Equation (106): For the fourth equation, use the expression of C_{rline} and D_{rline} in (23), and the equations in Lemma 1, to find that:

$$\begin{aligned} u_{sf}(t) &= C_{rline} x(t) - C_{rline} x_0 \\ &= C_{rline} x(t) + D_{sf} D_{c_1} C_{c_2p} x_{c_2p0} \\ &= C_{rline} x(t) + D_{rline} r_0 \end{aligned} \tag{110}$$

Therefore, all the equations of systems (22) and (27) are equivalent. This proves that systems (22) and (27) are equivalent under state transformation $\hat{x}(t) = x(t) - x_0$.

REFERENCES

[1] R H Munnig Schmidt, G Schitter, A Rankers, and J van Eijk. *The design of high performance mechatronics: high-tech functionality by multidisciplinary system integration (2nd revised edition)*, volume 2. IOS Press, Amsterdam, 2014.

[2] Alfonso Baños and Antonio Barreiro. *Reset Control Systems*. Springer London, London, 2012.

[3] Shih-Kang Kuo, Ximin Shan, and Chia-Hsiang Menq. Large travel ultra precision xy-/spl theta/motion control of a magnetic-suspension stage. *IEEE/ASME transactions on mechatronics*, 8(3):334–341, 2003.

[4] Shih-Kang Kuo and Chia-Hsiang Menq. Modeling and control of a six-axis precision motion control stage. *IEEE/ASME transactions on Mechatronics*, 10(1):50–59, 2005.

[5] Samir Mittal and Chia-Hsiang Menq. Precision motion control of a magnetic suspension actuator using a robust nonlinear compensation scheme. *IEEE/ASME Transactions on Mechatronics*, 2(4):268–280, 1997.

[6] Ximin Shan, Shih-Kang Kuo, Jihua Zhang, and Chia-Hsiang Menq. Ultra precision motion control of a multiple degrees of freedom magnetic suspension stage. *IEEE/ASME Transactions on mechatronics*, 7(1):67–78, 2002.

[7] J. C. Clegg. A nonlinear integrator for servomechanisms. *Transactions of the American Institute of Electrical Engineers, Part II: Applications and Industry*, 77(1):41–42, 7 1958.

[8] Isaac Horowitz and Patrick Rosenbaum. Non-linear design for cost of feedback reduction in systems with large parameter uncertainty. *International Journal of Control*, 21(6):977–1001, 1975.

[9] Leroy Hazeleger, Marcel Heertjes, and Henk Nijmeijer. Second-order reset elements for stage control design. In *Proceedings of the American Control Conference*, volume 2016-July, pages 2643–2648. Institute of Electrical and Electronics Engineers Inc., 7 2016.

[10] Niranjan Saikumar, Rahul Kumar Sinha, and S. Hassan Hosseinnia. 'Constant in Gain Lead in Phase' Element-Application in Precision Motion Control. *IEEE/ASME Transactions on Mechatronics*, 24(3):1176–1185, 6 2019.

[11] Nima Karbasizadeh and S. Hassan HosseinNia. Continuous reset element: Transient and steady-state analysis for precision motion systems. *Control Engineering Practice*, 126:105232, 2022.

[12] Nima Karbasizadeh, Niranjan Saikumar, and S. Hassan HosseinNia. Fractional-order single state reset element. *Nonlinear Dynamics*, 2021.

[13] Duarte Valério, Niranjan Saikumar, Ali Ahmadi Dastjerdi, Nima Karbasizadeh, and S. Hassan HosseinNia. Reset control approximates complex order transfer functions. *Nonlinear Dynamics*, 97(4):2323–2337, 9 2019.

[14] Qian Chen, Yossi Chait, and CV Hollot. Analysis of reset control systems consisting of a fore and second-order loop. *J. Dyn. Sys., Meas., Control*, 123(2):279–283, 2001.

[15] O Beker, CV Hollot, Q Chen, and Y Chait. Stability of a reset control system under constant inputs. In *Proceedings of the 1999 American Control Conference (Cat. No. 99CH36251)*, volume 5, pages 3044–3045. IEEE, 1999.

[16] Yuhang Zheng, Y Chait, CV Hollot, M Steinbuch, and M Norg. Experimental demonstration of reset control design. *Control Engineering Practice*, 8(2):113–120, 2000.

[17] S Hassan HosseinNia, Inés Tejado, and Blas M Vinagre. Basic properties and stability of fractional-order reset control systems. In *2013 European Control Conference (ECC)*, pages 1687–1692. IEEE, 2013.

[18] S Hassan HosseinNia, Inés Tejado, and Blas M Vinagre. Fractional-order reset control: Application to a servomotor. *Mechatronics*, 23(7):781–788, 2013.

[19] S Hassan HosseinNia, Inés Tejado, Daniel Torres, Blas M Vinagre, and Vicente Feliu. A general form for reset control including fractional order dynamics. *IFAC Proceedings Volumes*, 47(3):2028–2033, 2014.

[20] Orhan Beker, C. V. Hollot, Yossi Chait, and Huaizhong Han. Fundamental properties of reset control systems. *Automatica*, 40(6):905–915, 6 2004.

[21] O. Beker, C. V. Hollot, and Y. Chait. Plant with integrator: An example of reset control overcoming limitations of linear feedback. *IEEE Transactions on Automatic Control*, 46(11):1797–1799, 11 2001.

[22] Daowei Wu, Guoxiao Guo, and Youyi Wang. Reset integral-derivative control for hdd servo systems. *IEEE Transactions on Control Systems Technology*, 15(1):161–167, 2006.

[23] Niranjan Saikumar, Duarte Valerio, and S. Hassan Hosseinnia. Complex order control for improved loop-shaping in precision positioning. In *Proceedings of the IEEE Conference on Decision and Control*, volume 2019-December, pages 7956–7962. Institute of Electrical and Electronics Engineers Inc., 12 2019.

[24] Chengwei Cai, Ali Ahmadi Dastjerdi, Niranjan Saikumar, and S Hassan HosseinNia. The optimal sequence for reset controllers. In *2020 European Control Conference (ECC)*, pages 1826–1833. IEEE, 2020.

[25] P. W.J.M. Nuij, O. H. Bosgra, and M. Steinbuch. Higher-order sinusoidal input describing functions for the analysis of non-linear systems with harmonic responses. *Mechanical Systems and Signal Processing*, 20(8):1883–1904, 11 2006.

[26] Nima Karbasizadeh, Ali Ahmadi Dastjerdi, Niranjan Saikumar, Duarte Valerio, and S. Hassan HosseinNia. Benefiting from Linear Behaviour of a Nonlinear Reset-based Element at Certain Frequencies. 4 2020.

[27] Qian Chen. *Reset control systems: Stability, performance and application*. University of Massachusetts Amherst, 2000.

[28] Yuqian Guo, Lihua Xie, and Youyi Wang. *Analysis and Design of Reset Control Systems*. Institution of Engineering and Technology, 2015.

[29] Niranjan Saikumar, Kars Heinen, and S. Hassan HosseinNia. Loop-shaping for reset control systems: A higher-order sinusoidal-input describing functions approach. *Control Engineering Practice*, 111, 6 2021.

[30] Q. Chen, C. V. Hollot, Y. Chait, and O. Beker. On reset control systems with second-order plants. In *Proceedings of the American Control Conference*, volume 1, pages 205–209. IEEE, 2000.

5

Conclusions

The ever-increasing demands on controller performance currently force the high-tech industry to transition to nonlinear control. These controllers are not limited by the waterbed effect and Bode's phase/gain relation. Reset control is a widespread implementation of nonlinear control since it is compatible with loop-shaping and PID control. The main advantage of reset control lies in the reduction of phase lag, which can be used to increase damping. However, the damping in reset control systems also depends on the controller configuration. For instance, additional damping can be realized by locating a lead element before a reset element instead of after the reset in a CgLp. How the sequence of control elements influences, a reset system's transient response is not understood well. By developing an analytical method for analyzing the damping of a reset system instead of a numerical one, the influence of controller configuration on damping could be better understood and used to improve the transient performance of reset control systems.

Therefore, this thesis aims to develop an analytical approach to analyze the damping of the transient response in reset control systems with mass plants. The analytical step response was retrieved for reset control systems with a mass plant. The derived step response expression is valid for systems with at least one integrator, a diagonalizable system matrix, and all distinct eigenvalues. It can be used to analyze the realization of damping in the transient response.

In Section 4, two methods to analyze damping are proposed. First, the amount of damping can be determined by splitting the step response into oscillatory and exponential components and analyzing their corresponding coefficients. The faster the oscillatory step coefficients are reduced, the more damped the system will be. Furthermore, the slower the dominant exponential terms in the step response are, the slower and more damped the response will be.

Secondly, the amount of damping can be determined by analyzing the power and energy expressions. The damping in reset control systems can be expressed as the dissipation of the plant's energy. The earlier the controller can dissipate the initial plant's energy, the more damping the controller provides. If the controller can dissipate all energy before the reference is reached, overshoot can be prevented. Energy is dissipated when a controller applies negative power to a mass plant. Initially, the controller needs to decelerate the response to provide damping. One can analyze the damping by evaluating the coefficients of the oscillatory and exponential components of the acceleration response.

Oscillations in acceleration and power can lead to an increase in energy, which removes some damping provided earlier. Therefore, the faster the oscillatory acceleration coefficients are reduced, the more damping is provided. Furthermore, the slower the dominant exponential terms with negative coefficients of the acceleration response are, the longer damping will be provided.

These two approaches can be used to analyze the damping of the transient response in reset control systems analytically. Thereby enabling a more detailed analysis of the damping of the step response.

Finally, it was shown that the step response and power methods could approximate the amount of damping in the step response for a CgLp-PID controller with a mass plant. The damping in this controller can be optimized by placing the lead element before the reset in the CgLp. The increased

damping is mainly caused by a more significant reduction of the oscillatory content in both step and energy methods. The oscillation reduction depends on the magnitude of the higher-order harmonics at the oscillation frequency. The more lead is before the reset element, the more the higher-order harmonics and the oscillations are reduced.

6

Recommendations

The analytical approach developed in this thesis helps analyze the transient damping in reset control systems. This section discusses the research and provides recommendations for future work.

Validity of analytical solution The analytical analysis of the step response proposed in this thesis is only valid for reset control systems where the linear part of the system after the reset element contains at least one integrator. For mass plants, this will generally be true. If more complex plants are considered, an additional integrator could be necessary for the solution to hold. More work is needed to change the analysis to account for systems without at least one integrator, like mass-spring-damper systems.

Inclusion of other inputs A step is the only input considered in this thesis since the focus was on the transient response of reset systems. More work is needed to solve reset systems with other input functions analytically.

Tuning guidelines for transient performance This thesis proposes an approach to damping analysis. However, guidelines on how to use the analysis to tune controllers are not included. More work is needed to develop novel tuning guidelines for controller parameters, sequences, and reset instances to improve the transient performance in reset systems.

Dependence of damping on frequency response The connection between the frequency response and the damping of a reset system has yet to be fully understood. The phase margin primarily determines the damping. However, the higher-order harmonics also influence damping. For the CgLp-PID system introduced in Section 4, it was shown that the reduction of the higher-order harmonics at a specific oscillation frequency provides damping to the reset system. A more general and rigid theory needs to be formulated on how the damping is related to the higher-order frequency response in reset control systems.

Damping analysis of stable reset systems with unstable BLS The analytical solution of the reset systems does not require the reset system to have a stable base linear system. However, the proposed damping analysis methods require the BLS to be stable. The analytical expressions could be used to develop an approach to analyze the damping in reset systems with unstable BLS.

Stability analysis Finally, the analytical solution of the step response could provide a novel way to define the stability of reset control systems. If convergence of the step response is proven, stability can be determined from the analytical solution. Especially the analysis of the system's behavior during resets is of interest. Furthermore, note that the analytical derivation of the step response does not require the system to be BLS stable. It could be particularly interesting if stable reset systems with unstable BLS could be included in a stability analysis since the H_β stability condition cannot be used to prove the stability of these systems [16].

Bibliography

[1] Alfonso Baños and Antonio Barreiro. *Reset Control Systems*. Springer London, London, 2012.

[2] R H Munnig Schmidt, G Schitter, A Rankers, and J van Eijk. *The design of high performance mechatronics: high-tech functionality by multidisciplinary system integration (2nd revised edition)*, volume 2. IOS Press, Amsterdam, 2014.

[3] J. C. Clegg. A nonlinear integrator for servomechanisms. *Transactions of the American Institute of Electrical Engineers, Part II: Applications and Industry*, 77(1):41–42, 7 1958.

[4] Isaac Horowitz and Patrick Rosenbaum. Non-linear design for cost of feedback reduction in systems with large parameter uncertainty. *International Journal of Control*, 21(6):977–1001, 1975.

[5] Leroy Hazeleger, Marcel Heertjes, and Henk Nijmeijer. Second-order reset elements for stage control design. In *Proceedings of the American Control Conference*, volume 2016-July, pages 2643–2648. Institute of Electrical and Electronics Engineers Inc., 7 2016.

[6] Niranjan Saikumar, Rahul Kumar Sinha, and S. Hassan Hosseinnia. 'Constant in Gain Lead in Phase' Element-Application in Precision Motion Control. *IEEE/ASME Transactions on Mechatronics*, 24(3):1176–1185, 6 2019.

[7] Nima Karbasizadeh and S. Hassan HosseinNia. Continuous reset element: Transient and steady-state analysis for precision motion systems. *Control Engineering Practice*, 126:105232, 2022.

[8] Nima Karbasizadeh, Niranjan Saikumar, and S. Hassan HosseinNia. Fractional-order single state reset element. *Nonlinear Dynamics*, 2021.

[9] Duarte Valério, Niranjan Saikumar, Ali Ahmadi Dastjerdi, Nima Karbasizadeh, and S. Hassan HosseinNia. Reset control approximates complex order transfer functions. *Nonlinear Dynamics*, 97(4):2323–2337, 9 2019.

[10] Qian Chen, Yossi Chait, and CV Hollot. Analysis of reset control systems consisting of a fore and second-order loop. *J. Dyn. Sys., Meas., Control*, 123(2):279–283, 2001.

[11] O Beker, CV Hollot, Q Chen, and Y Chait. Stability of a reset control system under constant inputs. In *Proceedings of the 1999 American Control Conference (Cat. No. 99CH36251)*, volume 5, pages 3044–3045. IEEE, 1999.

[12] Yuhang Zheng, Y Chait, CV Hollot, M Steinbuch, and M Norg. Experimental demonstration of reset control design. *Control Engineering Practice*, 8(2):113–120, 2000.

[13] S Hassan HosseinNia, Inés Tejado, and Blas M Vinagre. Basic properties and stability of fractional-order reset control systems. In *2013 European Control Conference (ECC)*, pages 1687–1692. IEEE, 2013.

[14] S Hassan HosseinNia, Inés Tejado, and Blas M Vinagre. Fractional-order reset control: Application to a servomotor. *Mechatronics*, 23(7):781–788, 2013.

[15] S Hassan HosseinNia, Inés Tejado, Daniel Torres, Blas M Vinagre, and Vicente Feliu. A general form for reset control including fractional order dynamics. *IFAC Proceedings Volumes*, 47(3):2028–2033, 2014.

[16] Orhan Beker, C. V. Hollot, Yossi Chait, and Huaizhong Han. Fundamental properties of reset control systems. *Automatica*, 40(6):905–915, 6 2004.

[17] O. Beker, C. V. Hollot, and Y. Chait. Plant with integrator: An example of reset control overcoming limitations of linear feedback. *IEEE Transactions on Automatic Control*, 46(11):1797–1799, 11 2001.

[18] Daowei Wu, Guoxiao Guo, and Youyi Wang. Reset integral-derivative control for hdd servo systems. *IEEE Transactions on Control Systems Technology*, 15(1):161–167, 2006.

[19] Niranjan Saikumar, Duarte Valerio, and S. Hassan Hosseinnia. Complex order control for improved loop-shaping in precision positioning. In *Proceedings of the IEEE Conference on Decision and Control*, volume 2019-December, pages 7956–7962. Institute of Electrical and Electronics Engineers Inc., 12 2019.

[20] Chengwei Cai, Ali Ahmadi Dastjerdi, Niranjan Saikumar, and S Hassan HosseinNia. The optimal sequence for reset controllers. In *2020 European Control Conference (ECC)*, pages 1826–1833. IEEE, 2020.

A

List of symbols

Table A.1 provides a list of relevant symbols and a description. The presented symbols are introduced in this work. The more common symbols are not included in this list.

Table A.1: List of symbols.

Symbol	Description
C_1	Linear controller before the reset element.
C_2	Linear controller after the reset element.
C_2P	Linear controller after the reset element combined with the plant.
n	Total number of states of the reset control system.
n_1	Number of states of LC_1.
n_2	Number of states of LC_2P.
n_{pair}	Number of complex eigenvalue pairs of system matrix A_{cl}.
n_{real}	Number of real eigenvalues of system matrix A_{cl}.
Φ	State transition matrix.
α_j	Real part of the j-th complex eigenvalue pair of the system matrix A_{cl}.
β_j	Imaginary part of the j-th complex eigenvalue pair of the system matrix A_{cl}.
a_{kq}	k,q-th element of V containing the eigenvalues of the system matrix A_{cl}.
b_{ql}	q,l-th element of the inverse of V containing the eigenvalues of the system matrix A_{cl}.
$\sigma_{kl,j}$	Real part of $a_{kj}b_{jl}$ which is related to the j-th complex eigenvalue pair of the system matrix A_{cl}.
$\tau_{kl,j}$	Imaginary part of $a_{kj}b_{jl}$ which is related to the j-th complex eigenvalue pair of the system matrix A_{cl}.
c_{y_I}	Coefficients of the step response attributed to the complex eigenvalue pairs of the system matrix A_{cl}.
$c_{y_{I(2k-1)(2k)}}$	Coefficient of the oscillatory component of the step response attributed to complex eigenvalue pair k.
ψ	Phase shift of sine term through the combination of sine and cosine terms in the step response.
c_{y_R}	Coefficients of the step response attributed to the real eigenvalues of the system matrix.
ω_l	Lead location parameter in CgLp-PID. Determines how much lead is before/after the reset element.

B

Validation of analytic step response derivation

In this appendix, the analytic step response found in 4 is validated by comparing the response to a simulated version of the same system. Consider a PI-CgLp controller, controlling a mass plant. In this controller, the derivative part of a conventional PID is replaced by a CgLp-element using a GFORE and a 1^{st} order lead element as introduced by [6]. The order of application of the control elements influences the response of the system [20]. In this example, the configuration given in Figure B.1 is considered. Here, the Lead element is in front the reset element. The PI controller and plant are after the reset element. Call this system the Lead-Reset-Lag (LRL) configuration.

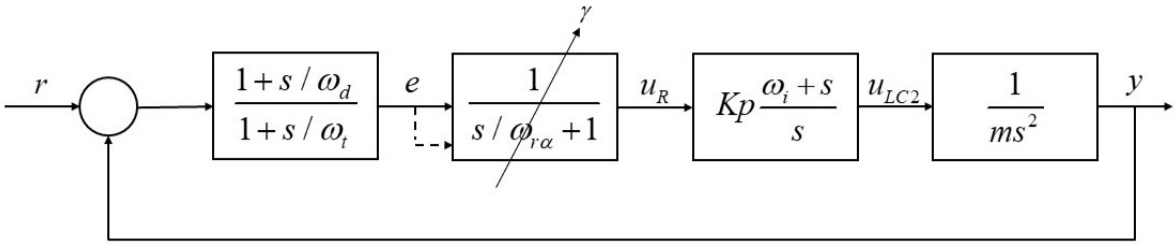

Figure B.1: Lead-Reset-Lag configuration of PI-CgLp & mass plant.

The behavior of the controller and plant for a constant reference input can be described analytically as introduced in Section 4. Then, the system can be described mathematically by B.1-B.6.

$$\begin{cases} \dot{\hat{x}} = A_{cl}\hat{x}(t), & \text{if} \quad C_{rline}\hat{x}(t) \neq 0 \\ \hat{x}(t^{+}) = \hat{A}_{\rho}\hat{x}(t), & \text{if} \quad C_{rline}\hat{x}(t) = 0 \\ y(t) = C_{cl}\hat{x}(t) + r_0 \end{cases} \tag{B.1}$$

In which,

$$A_{cl} = \begin{bmatrix} -\omega_{r\alpha} & \omega_{r\alpha} & 0 & 0 & -\omega_{r\alpha}\frac{\omega_t}{\omega_d} \\ 0 & -\omega_t & 0 & 0 & -\omega_t(1-\frac{\omega_t}{\omega_d}) \\ \frac{k_p\omega_i}{m} & 0 & 0 & 0 & 0 \\ \frac{k_p}{m} & 0 & 1 & 0 & 0 \\ 0 & 0 & 0 & 1 & 0 \end{bmatrix} \tag{B.2}$$

$$C_{cl} = \begin{bmatrix} 0 & 0 & 0 & 0 & 1 \end{bmatrix} \tag{B.3}$$

$$C_{rline} = \begin{bmatrix} 0 & 1 & 0 & 0 & -\frac{\omega_t}{\omega_d} \end{bmatrix} \tag{B.4}$$

$$\hat{x}(t) = \begin{bmatrix} \hat{x}_r & \hat{x}_{Lead} & \hat{x}_{PIplant} \end{bmatrix}^T \tag{B.5}$$

$$\hat{A}_\rho = \begin{bmatrix} \gamma & 0 \\ 0 & I^{4\times4} \end{bmatrix} \tag{B.6}$$

The state $\hat{x}(t)$ is the result of state transformation $\hat{x}(t) = x(t) - x_0$. Here, $x(t)$ contains the original states of the system and x_0 is given by B.7.

$$x_0 = \begin{bmatrix} 0 & 0 & 0 & 0 & r_0 \end{bmatrix}^T \tag{B.7}$$

The bandwidth ω_c is chosen to be at 100 Hz. The rest of the controller is tuned according to the guidelines in [6]. The controller and plant parameters can be found in Table B.1.

Table B.1: Controller parameters PI-CgLp.

Symbol	Value
ω_c	100 Hz
ω_i	ω_c/10
ω_d	ω_c/4
ω_t	6ω_c
γ	0
$\omega_{r\alpha}$	ω_d/1.62
K_p	2.2e6
m	5

For these parameters, the eigenvalues of system matrix A_{cl} consist of 1 pair of complex eigenvalues and 3 real eigenvalues, see B.8

$$\lambda = \begin{bmatrix} \alpha + \beta i \\ \alpha - \beta i \\ -3838.2 \\ -149.9 \\ -62.5 \end{bmatrix}, \alpha = 91.9, \beta = 526.1 \tag{B.8}$$

Note that the BLS of this system is unstable since 2 eigenvalues have a positive real part. A_{cl} has five distinct non-zero eigenvalues, A_{cl} will be diagonalizable. Moreover, the system in Figure B.1 contains three integrators after the reset element and can be written in observable canonical form. Therefore, the analytic step response can be found using the derivation in Section 4. The analytic expression of the step response can be seen in B.9-B.29.

$$y_{LRL}(t) = 1 + \sum_{l=1}^{5} \Phi(t - t_i)\hat{x}_l, \qquad t \in \langle t_i, t_{i+1}] \tag{B.9}$$

In which,

$$\begin{aligned} \Phi_{5l}(t - t_i) = {} & 2e^{91.9(t-t_i)}[\sigma_{5l}\cos(526.1(t - t_i)) - \tau_{5l}\sin(526.1(t - t_i))] \\ & + a_{53}b_{3l}e^{-3838.2(t-t_i)} + a_{54}b_{4l}e^{-149.9(t-t_i)} + a_{55}b_{5l}e^{-62.5(t-t_i)} \end{aligned} \tag{B.10}$$

$$\sigma_{5l} = \begin{bmatrix} -0.0171 & -0.6545 & -1.53e-6 & 0.0002 & 0.4689 \end{bmatrix} \tag{B.11}$$

$$\tau_{5l} = \begin{bmatrix} -0.0053 & -0.3023 & -6.01e-7 & -0.0009 & 0.0132 \end{bmatrix} \tag{B.12}$$

$$a_{53}b_{3l} = \begin{bmatrix} -0.0007 & 0.0005 & 1.17e-9 & -4.48e-6 & 0.0172 \end{bmatrix} \tag{B.13}$$

$$a_{54}b_{4l} = \begin{bmatrix} 0.0349 & 1.3032 & 1.77e-6 & -0.0003 & 0.0399 \end{bmatrix} \tag{B.14}$$

$$a_{55}b_{5l} = \begin{bmatrix} 0.0001 & 0.0053 & 1.29e-6 & -0.0001 & 0.0050 \end{bmatrix} \tag{B.15}$$

To verify the validity of the analytic step response derivation, it is compared to a simulation of the step response of the same PI-CgLp system. The simulation is done with the use of Simulink. The original system is assumed to be initially at rest: $x(0) = 0$. Therefore, the initial state vector of the transformed system will be:

$$\hat{x}(0) = x(0) - x_0 = \begin{bmatrix} 0 & 0 & 0 & 0 & -r_0 \end{bmatrix}^T \tag{B.16}$$

For this example, consider $r_0 = 1$. In Figure B.2, both the simulation and the analytical version of the step response can be seen. As both simulation and analytical responses overlap, one can assume that the analytical expressions correctly describe this system.

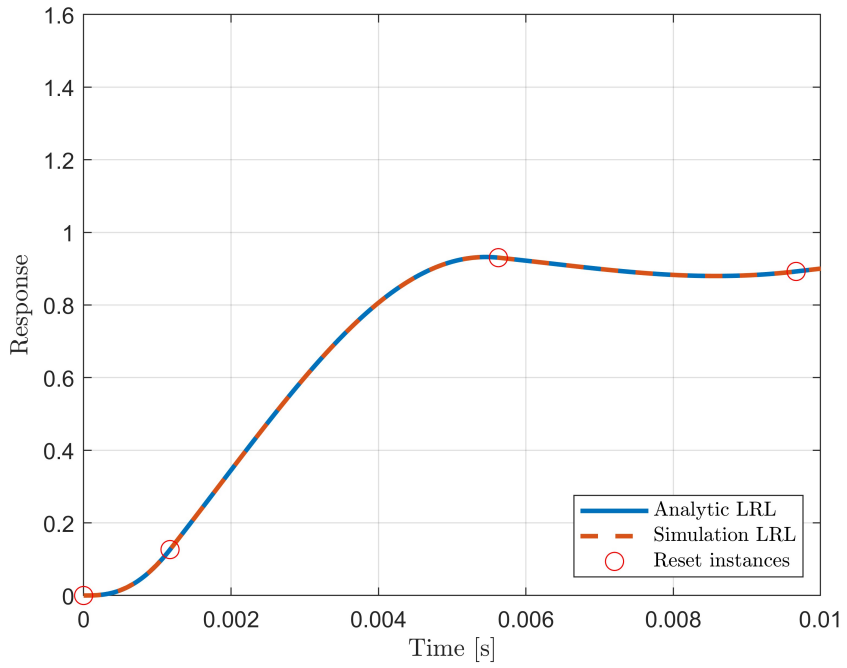

Figure B.2: Analytical and simulated step response of PI-CgLp in Lead-Reset-Lag configuration.

Moreover, consider the PI-CgLp system where the reset and lead element have been switched compared to Figure B.1. The new configuration can be seen in Figure B.3. This system is called the Reset-Lead-Lag (RLL) configuration.

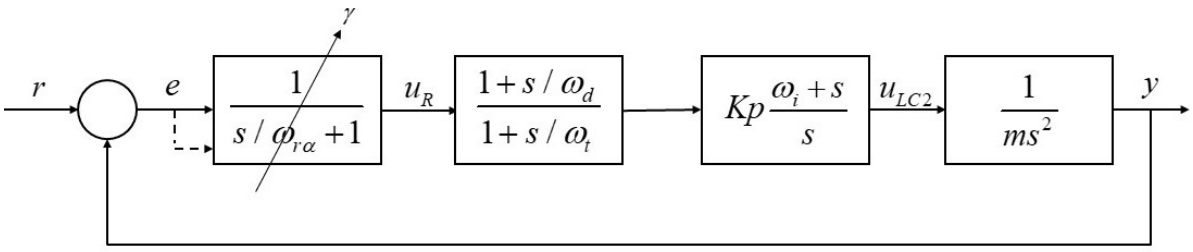

Figure B.3: Reset-Lead-Lag configuration of PI-CgLp & mass plant.

Similar to the LRL configuration, the RLL configuration can be described as a closed-loop system in B.1. The system matrices and vectors are provided in B.17-B.22

$$A_{cl} = \begin{bmatrix} -\omega_{r\alpha} & 0 & 0 & 0 & -\omega_{r\alpha} \\ \omega_t\left(1-\frac{\omega_t}{\omega_d}\right) & -\omega_t & 0 & 0 & 0 \\ \frac{k_p\omega_i\omega_t}{m\omega_d} & \frac{k_p\omega_i}{m} & 0 & 0 & 0 \\ \frac{k_p\omega_t}{m\omega_d} & \frac{k_p}{m} & 1 & 0 & 0 \\ 0 & 0 & 0 & 1 & 0 \end{bmatrix} \tag{B.17}$$

$$C_{cl} = \begin{bmatrix} 0 & 0 & 0 & 0 & 1 \end{bmatrix} \tag{B.18}$$

$$C_{rline} = \begin{bmatrix} 0 & 0 & 0 & 0 & 1 \end{bmatrix} \tag{B.19}$$

$$\hat{x}(t) = \begin{bmatrix} \hat{x}_r & \hat{x}_{Lead} & \hat{x}_{PIplant} \end{bmatrix}^T \tag{B.20}$$

$$\hat{A}_\rho = \begin{bmatrix} \gamma & 0 \\ 0 & I^{4\times4} \end{bmatrix} \tag{B.21}$$

$$x_0 = \begin{bmatrix} 0 & 0 & 0 & 0 & r_0 \end{bmatrix}^T \tag{B.22}$$

This controller has the same control parameters as the LRL configuration. The eigenvalues for both configurations are exactly the same. Therefore, the step response of the RLL PI-CgLp can be analytically described by B.23-**??**.

$$y_{RLL}(t) = 1 + \sum_{l=1}^{5} \Phi(t-t_i)\hat{x}_l, \qquad t \in \langle t_i, t_{i+1}]$$ (B.23)

In which,

$$\begin{aligned} \Phi_{5l}(t-t_i) = {} & 2e^{91.9(t-t_i)}[\sigma_{5l}\cos(526.1(t-t_i)) - \tau_{5l}\sin(526.1(t-t_i))] \\ & + a_{53}b_{3l}e^{-3838.2(t-t_i)} + a_{54}b_{4l}e^{-149.9(t-t_i)} + a_{55}b_{5l}e^{-62.5(t-t_i)} \end{aligned} \tag{B.24}$$

$$\sigma_{5l} = \begin{bmatrix} -0.3728 & -4.1e-10 & 1.48e-8 & 0.0001 & 0.0178 \end{bmatrix} \tag{B.25}$$

$$\tau_{5l} = \begin{bmatrix} -2.5568 & -10.0e-11 & -2.25e-7 & -1.29e-5 & 0.0618 \end{bmatrix} \tag{B.26}$$

$$a_{53}b_{3l} = \begin{bmatrix} 0.6806 & -1.71e-11 & 6.56e-8 & -0.0003 & 0.9662 \end{bmatrix} \tag{B.27}$$

$$a_{54}b_{4l} = \begin{bmatrix} 0.0617 & 4.90e-10 & -7.35e-8 & 1.10e-5 & -0.0017 \end{bmatrix} \tag{B.28}$$

$$a_{55}b_{5l} = \begin{bmatrix} 0.0032 & 3.47e-10 & -2.17e-8 & 1.36e-6 & -0.0001 \end{bmatrix} \tag{B.29}$$

In Figure B.4, both the step response of the LRL and RLL PI-CgLp's are graphed. They are compared to the simulated step response of the systems. The simulated and analytical step response do overlap for both cases. Which shows the validity of the analytical expression of the step response found in Section 4.

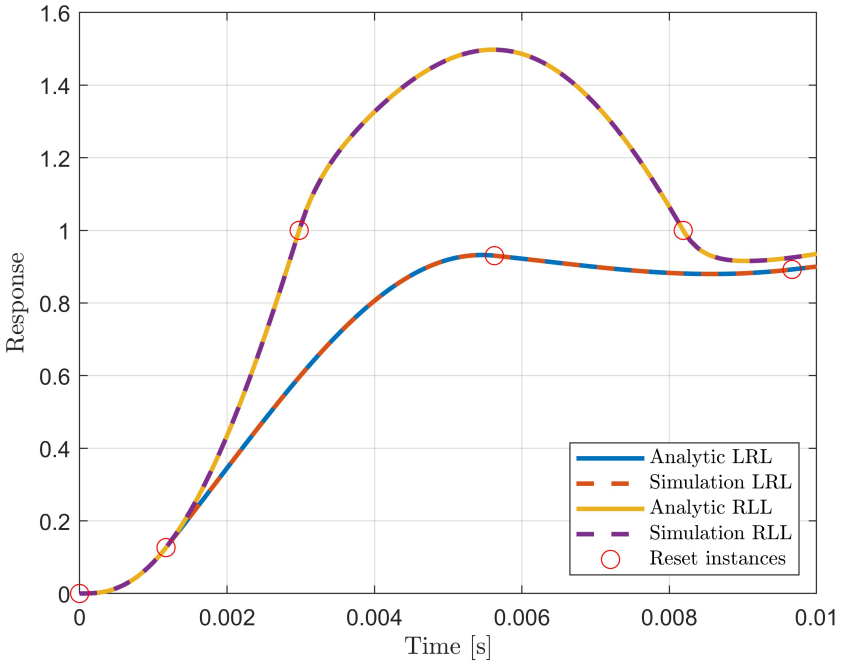

Figure B.4: Analytical and simulated step response of PI-CgLp in LRL and RLL configuration.

C

Matlab files

In this appendix, the most relevant matlab functions are provided:

- *Step_Reset_Analytic_TFBased.m* calculates the response of a reset control system to a step input based on the analytical expressions found in Section 4. Here the system needs to be provided to the function by entering the control elements separately.
- *Step_Reset_Analytic_paramBased.m* calculates the response of a reset control system to a step input based on the analytical expressions found in Section 4. Here the response parameters are provided to the function.
- *integration_analyticStep.m* calculates the response of a reset control system to a step input.
- *state_function.m* calculates the state values $x(t)$ based on the eigenvalues and vectors of A_{cl}.

C.1. Step_Reset_Analytic_TFBased.m

```
function [results,param_struct] = Step_Reset_Analytic_TFBased(LC1,RC,LC2P,SF,Arho,r0,t_start,t_stop,steps,reset_mode,t_reset_set_mode,t_reset_set)
    % Author: Mees Vanderbroeck, 2022
    % Function to find the step response of a reset control system

    % The reset control system is defined as follows:
    %      +     e              rout      u
    % ref --->  ---> LC1 -------> RC ---> LC2 ---> Plant ---> y
    %          ^            --SF--^                  |
    %       -  |                                     |
    %           -------------------------------------

    % LC1:      Linear controller before reset element transfer function
    % SF:       Shaping filter transfer function
    % RC:       Reset element (reset based on output LC1) state space
    % LC2:      Linear controller after reset element transfer function
    % Plant:    Plant transfer function

    % If system does not contain LC1, SF, or LC2, provide 0 as input

    % Other inputs:
    % - Arho:   Reset matrix
    % - r0: height of step input
    % - t_start: start time
    % - t_stop: stop time
    % - steps: integration steps
    % - reset_mode: 0 - no reset, 1 - reset
    % - t_reset_set_mode: 0 - reset line, 1 - predetermined reset,
    %                     2 - reset line & predetermined reset
    % - t_reset_set: predetermined set of reset instances

    % Outputs:
    % - results: contains step response data of system
    % - param_struct: contains all response and system parameters

    % CL_matrices provides the closed-loop form of the reset control system
    [A_cl,C_rline,Arhotot,x0unit] = CL_matrices(LC1,RC,LC2P,SF,Arho);

    % Eigenvalues_SysMatrix provides the eigenvalues and eigenvectors of
    % system matrix A_cl
    [V,Vinv,D,lambda_vec,nreal,nimag,npair,n] = Eigenvalues_SysMatrix(A_cl);

    % param_analyticStep calculates the response parameters of the step
    % response of the reset system. param_struct contains all response and
    % system parameters.
    [alpha_vec, beta_vec,sigma_matrix,tau_matrix,ab_matrix,param_struct] = param_analyticStep(D,V,Vinv,npair,n,nreal,nimag);

    % integration_analyticStep calculates the step response of the system
    % from the response parameters
    [x,xdot,xddot,t,plant_out,condition_val,x_reset,t_reset,idx_reset,x_t0] = integration_analyticStep(param_struct,C_rline,Arhotot,r0,x0unit*r0,...
                                                                                t_start,t_stop,steps,reset_mode,t_reset_set_mode,t_reset_set);
    plant_out_reset = x_reset(end,:)+r0*ones(1,length(t_reset));

    results.x = x;
    results.xdot = xdot;
    results.xddot = xddot;
    results.t = t;
    results.plant_out = plant_out;
    results.condition_val = condition_val;
    results.x_reset = x_reset;
    results.t_reset = t_reset;
    results.x0 = x0unit*r0;
    results.Crline = C_rline;
    results.Acl = A_cl;
    results.Arhotot = Arhotot;
    results.plant_reset = plant_out_reset;

    param_struct.Acl = A_cl;
    param_struct.Crline = C_rline;

end
```

Published with MATLAB® R2022a

C.2. Step_Reset_Analytic_paramBased.m

```
function results = Step_Reset_Analytic_paramBased(param_struct,r0,t_start,t_stop,steps,reset_mode,t_reset_set_mode,t_reset_set)
    % Author: Mees Vanderbroeck, 2022
    % Function to find the analytic step response of a reset control system
    % response parameters already calculated/known

    % Inputs:
    % - param_struct: contains all the response parameter values of the system
    %       * Acl, Crline, Arho, V, lambda, n, n_real, n_pair,
    %       * alpha, beta, sigma, tau, ab
    % - r0: height of step input
    % - t_start: start time
    % - t_stop: stop time
    % - steps: integration steps
    % - reset_mode: 0 - no reset, 1 - reset
    % - t_reset_set_mode: 0 - reset line, 1 - predetermined reset,
    %                     2 - reset line & predetermined reset
    % - t_reset_set: predetermined set of reset instances

    % Output:
    % Step response of reset system

    % Retrieving Crline, Arho, and x0 from parameter struct
    C_rline = param_struct.Crline; Arhotot = param_struct.Arhotot; x0 = param_struct.x0;

    % Integrating the response of the reset control system
    [x,xdot,xddot,t,plant_out,condition_val,x_reset,t_reset,idx_reset,x_t0,iter,cy,osci_content,cddy] = ...
        integration_analyticStep(param_struct,C_rline,Arhotot,r0,x0,t_start,t_stop,steps,reset_mode,t_reset_set_mode,t_reset_set);

    plant_out_reset = x_reset(end,:)+r0*ones(1,length(t_reset)); % Plant output during reset instances

    % Putting data in results struct
    results.x = x;
    results.xdot = xdot;
    results.xddot = xddot;
    results.t = t;
    results.plant_out = plant_out;
    results.condition_val = condition_val;
    results.x_reset = x_reset;
    results.t_reset = t_reset;
    results.x0 = x0;
    results.Crline = C_rline;
    results.Acl = param_struct.Acl;
    results.Arhotot = Arhotot;
    results.plant_reset = plant_out_reset;
    results.cy = cy;
    results.osci_content = osci_content;
    results.cddy = cddy;
end
```

Published with MATLAB® R2022a

C.3. integration_analyticStep.m

```
function [x,xdot,xddot,t,plant_out,condition_val,x_reset,t_reset,...
          idx_reset,x_t0,iter,cy,osci_content,cddy] ...
          = integration_analyticStep(param_struct,Crline,Arho,r0,x0,...
            t_start,t_sim,steps,reset_mode,t_reset_set_mode,t_reset_set)

    % Author: Mees Vanderbroeck, 2022
    % Function to find the analytical step response of reset control systems

    % Initializing
    t_reset = t_start;                      % Start time
    x_original_t0 = zeros(length(x0),1);    % Initial condition of original system
    t = linspace(t_start,t_sim,steps);      % Time vector
    dt = (t_sim-t_start)/(steps-1);         % Time step

    x_t0 = x_original_t0 - x0;              % Initial condition of zero-input system
    x_reset(:,1) = x_t0;                    % Set initial condition as first reset state
    idx_reset = [];                         % Index of reset
    prev_condval = Crline*x_t0;             % Initial reset condition

    % Set reset mode: reset on = true, reset off = false
    if reset_mode == true
        reset_mode = 1;
    else
        reset_mode = 0;
    end

    % Integration Loop
    for i = 1:length(t)
        x(:,i) = state_function(t(i),t_reset(end),x_reset(:,end),param_struct);                    % Position state calculation
        xdot(:,i) = statedot_function(t(i),t_reset(end),x_reset(:,end),param_struct);              % Velocity state calculation
        xddot(:,i) = stateddot_function(t(i),t_reset(end),x_reset(:,end),param_struct);            % Acceleration state calculation
        [condition_val(i),trigger,nreset] = ...
            reset_condition(Crline, x(:,i),t(i),dt,prev_condval,i,t_reset_set_mode,t_reset_set);    % Reset detection

        % Check whether a reset has been encountered
        % Reset set mode:
        %   - 0: resets determined by reset line
        %   - 1: resets determined by predefined set
        %   - 2: resets determined by reset line and predefined set
        if trigger == 1 && reset_mode == 1
            if t_reset_set_mode == 1                                                              % Check which set mode is active
                t_reset_new = t_reset_set(nreset)                                                 % Predefined reset has been encountered
            else
                if nreset == 0                                                                    % Check whether reset was predefined
                    [t_reset_new,findercount] =...
                        Reset_finder(t(i-1),t_reset(end),x_reset(:,end),Crline,param_struct);      % Interpolate to find reset instance
                else
                    t_reset_new = t_reset_set(nreset)                                             % Predefined reset had been encountered
                end
            end
            x_reset_new = Arho*state_function(t_reset_new,t_reset(end),x_reset(:,end),param_struct);    % Reset state calculation
            idx_reset = [idx_reset;i];                                                                  % Reset time index
            x_reset = [x_reset , x_reset_new];                                                          % Reset state
            t_reset = [t_reset , t_reset_new];                                                          % Reset instance
            x(:,i) = state_function(t(i),t_reset(end),x_reset(:,end),param_struct);                      % Position state calculation from new reset
            xdot(:,i) = statedot_function(t(i),t_reset(end),x_reset(:,end),param_struct);                % Velocity state calculation from new reset
            xddot(:,i) = stateddot_function(t(i),t_reset(end),x_reset(:,end),param_struct);              % Acceleration state calculation from new reset

        end

        % Show status of simulation
        if i == 1
            status = "Simulation started"
        elseif abs(i/steps - .25) < (1/2/steps) || abs(i/steps - .5) < (1/2/steps) || abs(i/steps - .75) < (1/2/steps)
            status = string(i/steps*100) + '% of simulation done'
        elseif i == steps
            status = "Simulation finished"
        end

        % Step response coefficients
        % specific to PID-CgLp, change to accomodate other systems
        cy(:,i) = [2*param_struct.sigma(7,:);-2*param_struct.tau(7,:);param_struct.ab(7,:,3);param_struct.ab(7,:,4);...
            param_struct.ab(7,:,5);param_struct.ab(7,:,6);param_struct.ab(7,:,7)]*x_reset(:,end);
        osci_content(i) = sqrt(cy(1,i)^2+cy(2,i)^2);

        % Acceleration coefficients calculation
        % specific to PID-CgLp, change to accomodate other systems
        cddy(1,i) = cy(1,i)*(param_struct.alpha^2-param_struct.beta^2)+2*param_struct.alpha*param_struct.beta*cy(2,i);
        cddy(2,i) = cy(2,i)*(param_struct.alpha^2-param_struct.beta^2)-2*param_struct.alpha*param_struct.beta*cy(1,i);
        for m = 3:7
            cddy(m,i) = param_struct.lambda(m)^2*cy(m,i);
        end

        % Output of system
        plant_out(i) = r0 + x(end,i);
        prev_condval = condition_val(i);

    end


end
```

C.4. state_function.m

```
function x = state_function(t,ti,x_ti,param_struct)
        % Author: Mees Vanderbroeck, 2022
        % Function to calculate the state values at a specific instance

        % Inputs:
        % - t: current time
        % - ti: last reset instance
        % - xti: state values at last reset instance
        % - param_struct: response and system parameter values

        % Output:
        % - x: state values at time t

        dt = t-ti;

        for k = 1:param_struct.n
            for l = 1:param_struct.n
                for j = 1:param_struct.npair
                    complex_terms(j) = 2*exp(param_struct.alpha(j)*dt)*(param_struct.sigma(k,l,j)*cos(param_struct.beta(j)*dt)...
                                                                        -param_struct.tau(k,l,j)*sin(param_struct.beta(j)*dt));
                end
                for r = param_struct.nimag+1:param_struct.n
                    real_terms(r,1) = param_struct.ab(k,l,r)*exp(param_struct.lambda(r)*dt);
                end
                Phi(k,l) = real(sum(complex_terms) + sum(real_terms));
            end
        end

        x = Phi*x_ti;
end
```

Published with MATLAB® R2022a